Earth-Science Reviews 185 (2018) 763–779

Contents lists available at ScienceDirect

Earth-Science Reviews

journal homepage: www.elsevier.com/locate/earscirev

Sub-magmatic arc underplating by trench and forearc materials in shallow subduction systems; A geologic perspective and implications

Mihai N. Ducea[a,b,*], Alan D. Chapman[c]

[a] University of Arizona, Department of Geosciences, Tucson, AZ 85721, United States
[b] Faculty of Geology and Geophysics, University of Bucharest, Bucharest, Romania
[c] Macalester College, Geology Department, St. Paul, MN 55105, United States

ARTICLE INFO

Keywords:
Tectonic underplating
Subduction systems
Arc magmatism
Exhumation

ABSTRACT

Sedimentary rock units originally formed in subduction trenches are often found tectonically underplated directly below magmatic arc crustal sections along some segments of the ancient convergent margin of the North American Cordillera. During and immediately after tectonic underplating - which takes place during ultra-shallow subduction - magmatic arcs shut off completely or migrate suddenly inboard, thus leaving the underplated sections in the new forearc of the subduction system. A good modern equivalent is found in Southern Mexico where the Cocos plate subducts at shallow angle under North America. The process is episodic and corresponds to events of sudden trench inboard migration relative to the upper plate. If the trench sequence was dominated by quartz-rich material, the exposed rocks are schists; they display an inverse pressure-temperature path, suggesting that the crust collapsed and were exhumed immediately after the completion of this ablative process (Salinas type). If rich in feldspar, the trench-derived metasedimentary rocks are gneisses and display evidence for thermal relaxation-related heating and in some cases, partial melting (Skagit type). Feldspar-rich rocks presumably have a higher strength that precludes a quick gravitational collapse of the section. In both cases, this process leads to the complete reorganization of the crust with the addition of melt fertile, first cycle sedimentary materials in the deep crust of subduction systems.

1. Introduction and problem setup

Major subduction and collisional convergent margins on Earth commonly accommodate shortening along fold and thrust belts. Subduction of an oceanic plate itself takes place along an enormous and long lived thrust fault. However, smaller thrust faults provide better insights into the mechanics and geometry of shortening. The best examples of such thrust systems are preserved in areas that underwent continental collision, such as the Alps or Himalayas, although they are found in subduction settings as well. The total amount of shortening accommodated by fold and thrust belts can be as much as 500–700 km for long lived convergent margins (DeCelles et al. 2002; Gotberg et al. 2010). This very common compressive structural style can easily bury sedimentary rocks to great crustal depths (> 30 km) where they undergo metamorphism and in some cases, partial melting.

Individual thrust faults accommodate a finite amount of displacement and are active over a fraction of the lifetime of the convergent margin. Newer faults propagate ether structurally downward leaving the fossil fault in the hanging wall of the thrust system (most of the time, also known as in-sequence thrusting) or vice-versa (less common). Consequently, underthrusting of shallow rocks into a deeper structural position along footwalls of thrust faults and subsequent abandonment of these masses in the hanging wall of later faults is an efficient lateral transport mechanism in collisional belts.

Subduction of oceanic plates follows, at least near the trenches, the geometry of all fold and thrust belts (Burg et al. 2013). The major difference presented by the fault representing the mega-subduction thrust fault is that in theory it is a structure that can accommodate infinite displacement and transport the footwall (the subducting plate) down into the deeper parts of the mantle along the same fault plane for long periods of time. In reality, the subduction megathrusts shift their position over time relative to the upper plate generating a set of sutures very much similar to continental fold and thrust belts; these are well documented near the trenches and in forearcs of subduction systems. If the migration of the mega-thrust is structurally downward and therefore outboard relative to the upper plate, the margin is said to be accreting. If the opposite is true, the margin is eroding (e.g. Park et al. 2002). Eroding margins are cannibalizing their accretionary wedge and

* Corresponding author at: University of Arizona, Department of Geosciences, Tucson, AZ 85721, United States.
E-mail address: ducea@email.arizona.edu (M.N. Ducea).

https://doi.org/10.1016/j.earscirev.2018.08.001
Received 3 May 2018; Received in revised form 18 July 2018; Accepted 1 August 2018
Available online 03 August 2018
0012-8252/

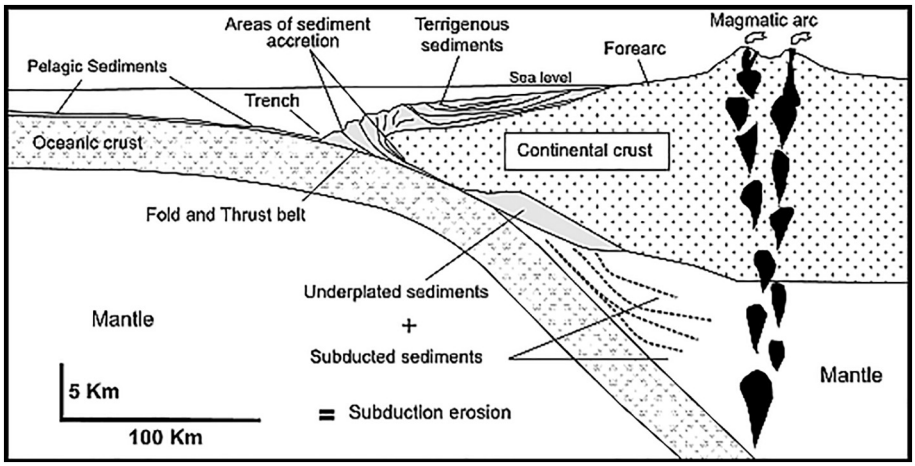

Fig. 1. Cross section through a subduction zone showing the main elements of the margin and the possible destination of sediment buried from the trench – sediment subduction and underplating. Some of the sedimentary budget also returns to upper plate via arc magmatism although that is generally a small percentage of subducted sedimentary material (from Ducea et al. 2004b).

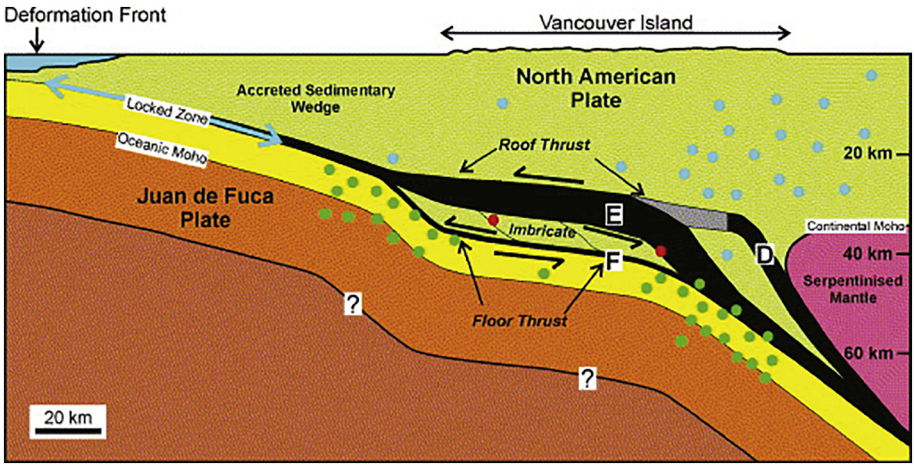

Fig. 2. From Calvert et al. (2006). Schematic cross-section normal to the Cascadia margin at the location of southern Vancouver Island. The E and F reflectors define the roof and floor thrusts respectively of a 100-km-wide duplex structure, beneath which the Juan de Fuca plate subducts. The D reflectors may also be part of the roof thrust, but have not yet been shown to be continuous with the E reflectors, as indicated by the grey region. Seismicity (green dots mark major earthquake locations) in the subducting slab occurs primarily where the top of the plate is inferred to steepen. Various blue and red dots are hypothetical locations of various earthquakes along this active structure. (For interpretation of the references to colour in this figure legend, the reader is referred to the web version of this article.)

in some cases forearcs and sending sediments downward with the megathrust. More than half of the modern trenches are eroding making this process rather significant (von Huene and Scholl, 1991, Clift and Vannucchi 2004, 2009, Scholl and von Huene 2007). In the simplest of explanations, the plausible destinations of trench-accumulated sediments are (Fig. 1): (1) in the trench, accreted, (2) subducted into the mantle, (3) accreted structurally to the bottom of the upper plate after initial downward transport and (4) return to the upper plate either via magmatism with partial melting of the downgoing sediment or some other form of solid-state or partially molten upward transport.

Global mass balance calculations on modern subduction settings show that most of these materials have to be retained in the upper plate of subduction systems (Clift and Vannucchi 2004) or else the overall mass of continental crust would be rapidly declining, an interpretation which is at odds with a variety of data for the Phanerozoic (Reymer and Schubert 1984); in Clift and Vannucchi's seminal paper (2004), the authors favor the return of large proportions of sediment via melting under magmatic arcs (Kay et al. 2005). A number of speculative models involving the convective or advective return of trench materials to the upper plate exist in the literature and they may well account for some return of materials eroded from the trench. Relamination refers to sedimentary diapirs lifting from the slab and being transported upwards either as solids or partially molten through the mantle wedge and being attached to the bottom of the upper plate crust (Behn et al. 2011). Partial melting of subducted sediment and ascent via arc magmas has been hypothesized for a while (Defant and Drummond 1990) and remains popular among some researchers (Kelemen et al. 2004) despite the evidence that sediment contribution appears to play a secondary to insignificant role in most Phanerozoic magmatic arcs (Ducea et al. 2015).

Geologic evidence points a more likely mechanism for transferring sedimentary materials at eroding subduction margins by duplexing along the major (subduction) thrust fault (Ducea et al. 2009) in a process that some refer to as tectonic underplating (a term which in the literature is not restricted to this process, but one that will be used below). Such geometries are commonly identified at depth under forearcs (Calvert et al. 2011) and evidence exists that trench-related materials can travel as far as 300 km inboard to be eventually duplexed under the magmatic arc of some subduction margins (Manea et al. 2013). Slivers of mantle may or may not be present in between the underplated rocks and the upper plate crustal materials at any given location.

Forearc and sub-arc duplexing are worth being introduced here with a well-studied modern example since it is the primary mechanisms by which tectonic underplating occurs. Perhaps the first discovery of underplated materials in modern forearc regions of subduction system (in seismic images) was made in the Aleutians by James Sample, Casey Moore and collaborators in the late 1980s (e.g. Moore et al. 1991). Fig. 2 (Calvert et al. 2006) exemplifies the mechanism of duplexing in the forearc of the North American Cordillera, near Vancouver island: the interpreted geologic cross section based on seismic data (Fig. 2) shows a series of abandoned faults (D and E) that were responsible for transferring the black labeled units from the downgoing plate onto the forearc of the upper plate while the active subduction megathrust (labeled F) migrates downward over time. Although here involving the mega-subduction thrust, this process of duplexing is geometrically no different than what structural geologists observe rather commonly in fold and thrust belts.

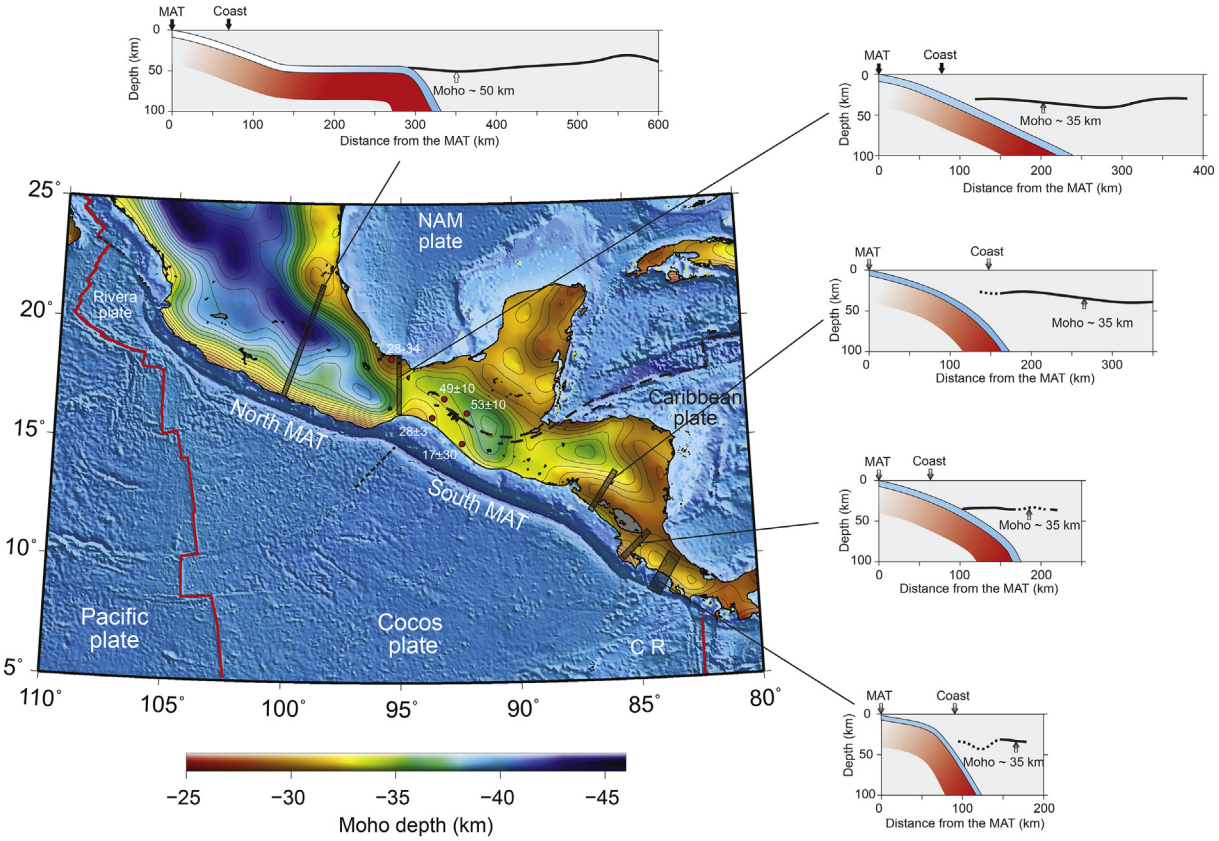

Fig. 3. Moho topography for Mexico and Central America (from Manea et al. 2013): Moho map is based on gravity GOCE data (Reguzzoni and Sampietro 2012). 2D profiles represent Moho and slab geometry and are based on seismic experiments (Dzierma et al. 2010; Melgar and Pérez-Campos 2011; Pérez-Campos et al. 2008). Red dots depict point Moho depth estimations from seismic experiments (Narcia-Lopez et al., 2004). White number labels represent depths and accuracies for large earthquakes recorded in the area. (For interpretation of the references to colour in this figure legend, the reader is referred to the web version of this article.)

Examples for tectonic underplating do exist in the geologic record and are best known in the North American Cordillera. The focus of this paper is a geologic review of some of these well-known examples. They will be examined below in an effort to distinguish end member types of tectonic underplating and their predicted thermal, structural and magmatic consequences. We show that underplated sections of the lower continental crust can proceed at large scale and have tremendous consequences on the composition and evolution of the continental crust during the orogenic event and after. We also draw the attention to the fact that this process is relatively difficult to be detected in the geologic record because it generates Barrovian metamorphism and not the high pressure/low temperature type normally expected to form as a result of oceanic subduction.

2. Recognizing a low-angle subdcution complex

The first fundamental question for those studying tectonic shuffling at subduction margins is what types of rocks can one expect to find as a result of this process? First, we will review how does one identify the products of “normal-angle” subduction in the geologic record, followed by a summary of ultra-shallow subduction and thus the expectations pertaining underplated rocks.

In normal subduction, for the most part, the critical element is the presence of high pressure/low temperature metamorphic products (Miyashiro 1973), which form along subducting plates (Hacker et al. 2003). This includes greenschists, blueschists and eclogite facies rocks, or at the least the presence of prehnite-pumpellyite facies rocks that may have undergone the early stages of that style of metamorphism. High pressure/ low temperature metamorphism is restricted to subducted plates because they are buried at high speeds typical for plate rates (centimeters a year) and the temperatures remain relatively low in those environments. Typically, such “subduction complexes,” of which the Franciscan Complex of California is a classic example, are found as mélanges in which metamorphosed rocks and deformed fragments of the oceanic lithosphere are found within matrices of less metamorphosed rocks (Hsu, 1968; Cloos 1982; Raymond 1984; Wakabayashi 2015) and block-in-matrix metamorphism predates the sedimentary age of the matrix (Ukar 2012). The origin of these complexes remains controversial (Wakabayashi 2015) and they were likely returned very fast along a subduction channel (Platt 1986; Cloos and Shreve 1988). A final key observation common to many subduction complexes is the presence of upsection/inboard increases in metamorphic grade and depositional age – so called “inverted field gradients,” as these trends are contrary to those expected for an intact section of rock in the earth (Ernst 1980; Peacock 1987). Inverted metamorphic and age gradients in subduction complexes are most readily explained by underthrusting of progressively younger slices beneath an upper plate that is cooling due to downward heat transfer (i.e. “subduction refrigeration,” Dumitru et al. 1991). To summarize, high-pressure/low-temperature metamorphism, inverted metamorphism, inverted depositional age patterns, and the presence of melange are hallmark features of “normal-angle” subduction complexes (Philpotts and Ague 2009).

Like “normal-angle” subduction complexes, shallow-angle subduction products also commonly exhibit downsection younging, upsection increases in metamorphic grade, and the presence of mélange. However, shallow-angle subduction assemblages (trench sediment plus the potential added presence of mafic/ultramafic material from fragments of the oceanic slab) are conveyed directly beneath recently active (i.e. hot) continental arcs, rather than coming into contact with the cold base of an accretionary wedge and/or forearc basin, as is the case for

"normal-angle" subduction complexes. As a result, shallow-angle subduction complexes are of a higher metamorphic grade than their normal-angle counterparts. Even a short geologic time (a few million years, e.g. 2–5 My) spent at depths of 20–30 km would result in the change of the metamorphic path from high pressure/low temperature to a Barrovian one (medium temperature and pressure), a more commonly encountered PTt pathway in orogenic areas. Consequently, metasedimentary rocks will become garnet-bearing schists and gneisses and have a metamorphic facies more commonly associated with continental collision or other dynamo-thermal orogenic situations (Philpotts and Ague 2009) not necessarily associated with subduction, even though they represent fundamentally trench and/or forearc derived materials. This is an important and commonly overlooked aspect of underplating which may have led to the under recognition of such rocks in the geologic record.

3. Southern Mexico – A modern example

Southern Pacific Mexico is an illustrative example of ultra-shallow subduction where the Cocos slab penetrates for hundreds of kilometers under the upper plate (North America)under its lower crust (Fig. 3) (Parolari et al. 2018). This feature is best observed at the longitude of Acapulco. Note that geometry changes progressively to a more normal angle of subduction to the east along the same subduction zone (Manea et al. 2013). The scale of experiment and type seismic data available here do not show the same level of detail seen in the Vancouver forearc example above (i.e. one cannot distinguish duplex structures within the upper plate with such data), but they do illustrate the potentially extensive interaction between the upper and lower plates along an unusually wide forearc. Note that there is no mantle section between the upper and lower plates for 300 km inboard of the trench, expect possibly a 4 km low velocity hydrous mantle between plates (Kim et al. 2013). The modern arc, the main Mexican arc in this case (or the Trans Mexican Volcanic Belt, Ferrari et al. 2012; Straub et al. 2011, 2015; Gomez Tuena et al., 2018) is located further to the east, where the slab begins steepening again and the Moho increases toward the back side of the subduction system (Fig. 3).

Perhaps the most important geologic feature of southern Mexico geology relevant to our discussion is that the Mesozoic to Cenozoic arc (including rocks as young as Oligocene and earliest Miocene) are found around the beach exposures of Pacific Mexico and offshore and only 20–30 km from the modern trench (Ducea et al. 2004a, 2004b). Clearly, much of the forearc and the trench of earlier Cenozoic have been removed. As it often is the case in such scenarios, there are two hypotheses: either the forearc was removed laterally (the Chortis block, found today to the east in Central America) or it was subducted-eroded with an evolving margin that developed into today's ultra-shallow subduction. The hypothesis of margin erosion by subduction is far more plausible (see Ducea et al. 2004b).

While this modern example typifies ultra-shallow subduction geometry, in which the slab interface moves inboard for hundreds of kilometers without cutting into mantle (lithosphere and asthenosphere), at face value does not require tectonic underplating. In other words, lower plate material need not get stuck under the and become part of the upper plate. On the other hand, it is known that the trench in this area is a severely retreating one for the past 25 My or possibly more; remnants of the Eocene to Miocene magmatic arc are found along the coastal exposures of Sierra Madre del Sur (Ducea et al. 2004a; Morán-Zenteno et al., 2018) with the modern Acapulco trench only 20–30 km outboard of the coast. A large fraction of the accretionary wedge and the forearc of the early to mid-Cenozoic subduction margin are missing and transported downward with the subducting slab. Low temperature thermochonology data (U-Th/He) document that only about 10% of the sediment eroded since the earliest Miocene of the Sierra Madre del Sur (the elevated forearc of this subduction system) is found in the trench today (Ducea et al. 2004b), the rest having been subducted away. It is unlikely that such a high flux of sedimentary material (corresponding to some 50–60 km^3/km My) was transferred to the deep mantle and most likely some was underplated. The Trans Mexican volcanic belt could have recycled some of that material magmatically (Straub et al. 2015) given the geochemical and isotopic composition of the arc, but probably not > 5% of the missing trench/forearc. Thus the great majority of eroded material from the forearc side is probably underplated at depth under mainland Mexico.

We suggest that ultra-shallow subduction episodes associated with massive trench retreat (so called erosive margins) like the Acapulco example presented here promote tectonic underplating. The Laramide shallow subduction event of the latest Cretaceous in North America (Saleeby 2003) was such an event in which the slab planed off ~30–45 km beneath the surface (Cheadle et al. 1986; Trehu and Wheeler 1987; Li et al. 1992; Malin et al. 1995; Magistrale and Zhou 1996; Grove et al. 2003b; Chapman et al. 2010; Jacobson et al. 2011; Porter et al. 2011) for hundreds of kilometers inboard from the trench and is the tectonic event responsible for the geologic examples reviewed below.

4. Relevant North American geologic examples

All examples presented below are found within the Cordilleran region of western North America (Fig. 4) and appear to be of similar age – latest Cretaceous to Paleocene. This corresponds to a time of regional shallow subduction, which is widely known as the Laramide orogeny (DeCelles 2004; Saleeby 2003; Liu 2015; Yonkee and Weil 2015). In the broadest of sense therefore, there is a clear link between shallow subduction and underplating in these examples although in detail, the magnitude of ultra-shallow subduction in the American west may have varied along the strike and many other details of the process may have been different from one described location to the other. We present the Southern California Allochton as the prime example of Laramide tectonic underplating, which left many individual exaplmes of schists and gneissic terranes structurally under native North America. Of the totality of the southern California examples, we focus on a few better studies examples, and among them, we particularly highlight the Salinia-schist of Sierra de Salinas example in central coastal California today.

Following the Californian examples, we also address some recently discovered underplated sections in the core of the Cascades area in the Pacific north west, in British Columbia, Alaska. Geologic knowledge in these more recently discovered examples is perhaps not as thorough as it is for the California examples which have been known for many decades. However, they demonstrate the continental scale of this process in the North American Cordillera and thus bolster the argument that this process is tectonically significant for continental evolution.

4.1. The Southern California Allochthon

4.1.1. Introduction and Sierra de Salinas-Salinian type example

Collectively, the southern California exposures make up the world's best example of a subduction complex underplated beneath the North American continent during the Laramide orogeny in the latest Cretaceous, a regionally significant episode of shallow subduction (DeCelles 2004). The local underplating is well known and studied regionally (e.g. Hall, 1991) but its larger scale significance with regard to subduction erosion and tectonic underplating remains under appreciated. There are 24 individual areas in southern and central California where North American upper plate crustal rocks commonly containing Cretaceous magmatic arc rocks are underlain by metasedimentary rocks deposited only a few million years before being emplaced at depth during the latest Cretaceous (Barth et al. 2003). The largest of the exposed areas are shown in a palinspastic reconstruction in black in Fig. 5. These pieces may not have belonged to precisely the same thrust sheet, since most likely there were several thrusts that were emplaced

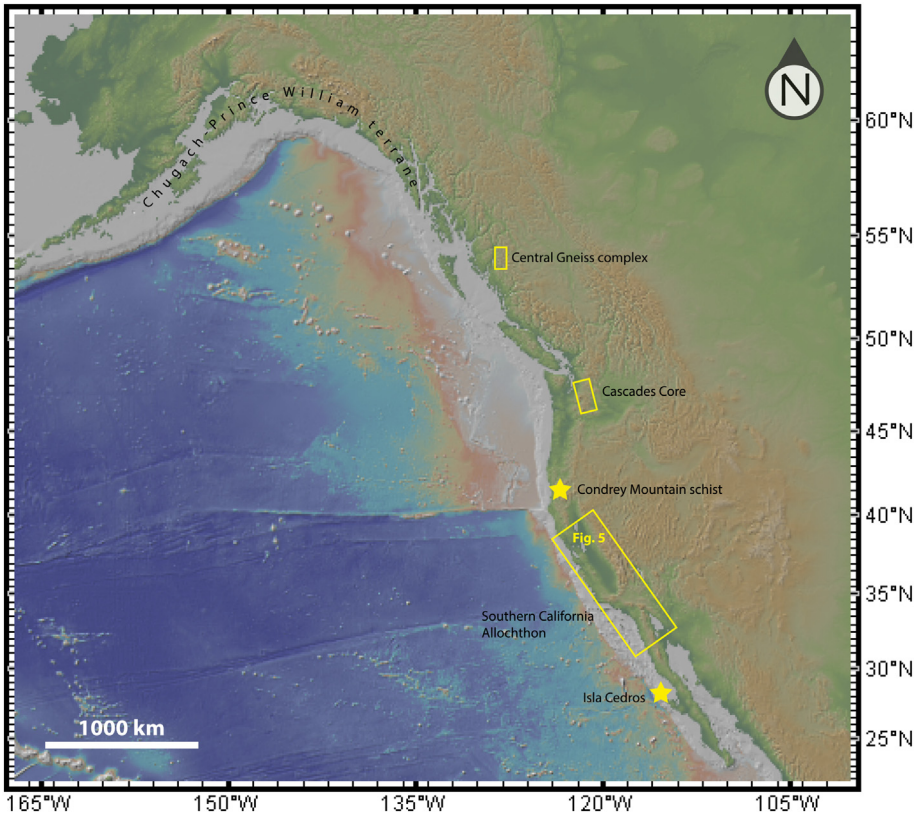

Fig. 4. General locations of the following areas described in text: the Southern California Allochthon (detailed in Fig. 5), the Cascades core, parts of the Central Gneiss Complex, the Chugach-Prince William terrane, Condrey Mountains schist and Islas Cedros (IC).

successively over several million years, but they probably represent the product of the same event or possibly two events in short succession (Saleeby 2003; Grove et al. 2003a; Liu et al. 2010). Cenozoic tectonism, extension in the greater Mojave region and/or the lateral displacement of part of southern California along the San Andreas fault, led to the fragmentation seen today. It is due to the more recent tectonism associated with the San Andreas fault that the Sierra de Salinas-Salinia area has been displaced some 300 km to the north relative to North America (and is exposed today in central coastal California) and not in southern California, its place of origin.

It is widely believed that much of the southern and central California areas near the San Andreas fault system extending into the Mojave region and western Arizona are underlain by equivalent schists emplaced during Laramide shallow subduction. Geophysical evidence further suggests that much of the sub Mojave region is underlain by materials similar to those exposed in the small windows of underplated rocks (Tape et al. 2009; Porter et al. 2011) although their vertical extension (down into the lower crust or perhaps closer to the modern Moho?) is debated. Lower plate metasedimentary rocks mixed with minor mafic and ultramafic materials are locally known as the Pelona, Rand, Orocopia, San Emigdio, and Sierra de Salinas schists and are found in footwall of thrust faults subsequently reactivated as normal faults.

The term Southern California allochthon (SCA) was used by Hall (1991) only for the central Californian Cretaceous magmatic arc block of Salinia, which is sitting atop of the Sierra de Salinas schist. The Sierra de Salinas/Salinian example is in some ways the best example of all of these exposures because the structure separating them appears to the original thrust fault (despite subsequent extension) (Kidder and Ducea 2006); we describe it here separately from the rest of the Californian example. We draw from this example heavily in this paper in part because of its next to ideal geologic preservation and because of our own experience working with it. Magmatic arc rocks equivalent to the ones on the Sierra Nevada arc or any other arc fragment of California (Kidder et al. 2003) sit separated by a major ductile fault called the Salinas shear zone (Ducea et al. 2007) atop of metamorphosed trench materials (Kidder and Ducea 2006) (Fig. 6) that were sedimentary only a few million years (Barth et al. 2003) before being buried and metamorphosed (Ducea et al. 2003a). The exposed ductile fault was about 30–35 km deep at the time of formation (Fig. 6). The arc stopped forming while it was being underplated with sediments at around 80 Ma and the entire section collapsed gravitationally a few million years after; as a result, Maastrichtian marine sediments unconformably overlie this deep crustal section (Fig. 7). As a result of that early collapse, about 30 km of crustal section were removed (Fig. 7 A, schematic W-E cross section); the transpressional late Cenozoic uplift of the Coast Ranges (Ducea et al. 2003c) further contributed to the present day geologic complexities in the Santa Lucia range (Fig. 7B).

The term allochthon was used to signify that the upper plate of the central California coastal Cretaceous magmatic arc assemblage (Salinia) appear to be transported westward > 180 km relative to the underlying subduction complex sediments (Franciscan and Sierra de Salinas rocks). The intervening forearc and parts of the arc are missing (Ducea et al. 2009; Jacobson et al. 2011; Chapman et al. 2016; Johnston et al. 2018). Some (Dickinson 1983; Dickinson et al. 2005; Jacobson et al. 2011) have argued that the truncation of the margin is due to trench-parallel left lateral slip, but palinspastic reconstructions indeed suggest that all of southern California's geology is shifted westward relative to the normal location of the magmatic arc to the north (see Hall and Saleeby 2013, for a review of many decades of regional research). The somewhat antiquated term “allochthon” is used here in conjunction with the southern California region; all of Southern California (and other belonging blocks moved to the north) floats westward on top of subducted/accreted or underplated trench and forearc materials. It is of course a relative term; relative to the upper plate, it is the schists that are allocthonous, i.e. they were displaced significantly inboard relative

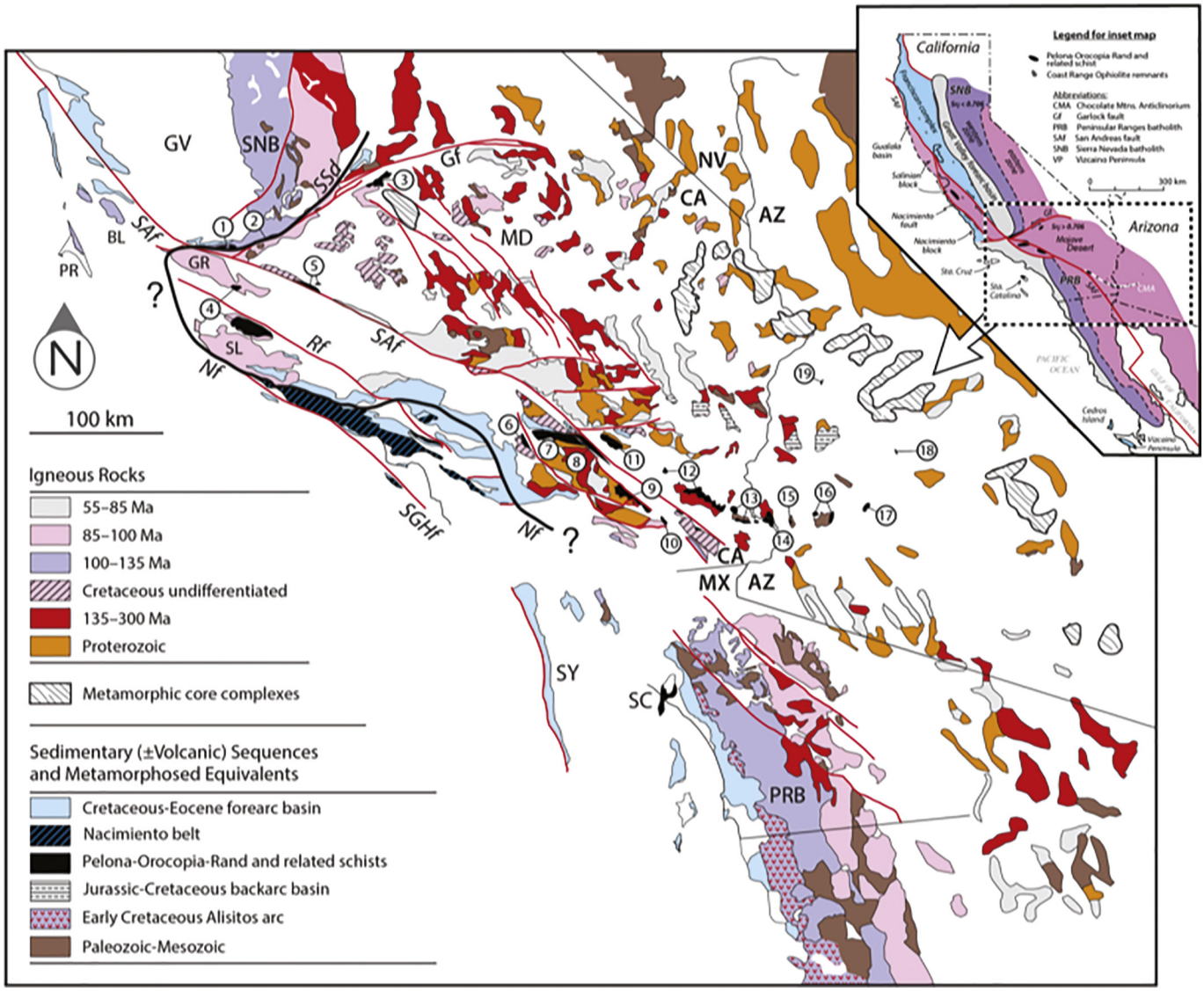

Fig. 5. Pre–San Andreas palinspastic reconstruction of southern California, SW Arizona, and NW Mexico after Grove et al. (2003a) and Jacobson et al. (2011). Inset showing present day configuration after Chapman et al. (2012). The main areas of southern and central California in which underplated schists and gneisses (black areas) are present structurally below North American upper plate rocks, many of which were parts of the subduction-related Cretaceous magmatic arc prior to the episode of underplating (modified after Chapman 2017). Numbered schist localities, all part of the Southern California Allochron: 1 – San Emigdio Mountains, 2 – Tehachapi Mountains, 3 – Rand Mountains, 4 – Sierra de Salinas/Salinia, 5 – Portal/Ritter ridges, 6 – Mount Pinos, 7 – Sierra Pelona, 8 – Blue Ridge, 9 – East Fork, 10 – San Gorgonio Pass, 11 – Orocopia Mountains, 12 – Chocolate Mountains, 13 – Picacho-Peter Kane Mountain/Gavilan Hills, 14 – Marcus Wash/Trigo Mountains/Yellow Narrows, 15 – Middle Mountains, 16 – Castle Dome Mountains, 17 – Neversweat Ridge, 18 – Cemetery Ridge, 19 – Plomosa Mountains. Abbreviations - BL: Ben Lomond Mountain; GR: Gabilan Range; GV: Great Valley; MD: Mojave Desert; PR: Point Reyes; PRB: Peninsular Ranges batholith; SC: Santa Catalina Island; SL: Santa Lucia Mountains; SNB: Sierra Nevada batholith; Fault abbreviations: Gf: Garlock; Nf: Nacimiento; Pf: Pastoria fault; Rf: Reliz- Rinconada; SAf: San Andreas; SGHf: San Gregorio–Hosgri; SSd: Southern Sierra detachment. A more detailed map of the Salinia/schist of the Sierra de Salina example is shown in Fig. 6 as an example of a typical such location. (For interpretation of the references to colour in this figure legend, the reader is referred to the web version of this article.)

to the upper plate arc.

The schist of Sierra de Salinas is equivalent to the Pelona, Orocopia, Rand, and Tehachapi/San Emigdio and other schists (Fig. 5), though the latter schists have not been displaced from southern California in Neogene time. Like the schist of Sierra de Salinas, which we use here as the main example of a locality of these types of materials in southern California, schist exposures occur as structural windows through tectonically overlying granitic rocks of the California magmatic arc and pre-batholithic gneissic rocks. The following is a brief overview of geologic relations found in some of the other classic exposures (divided into a northern and southern group of schists), as well as a newly discovered locality in Mexico.

4.1.2. Rand/San Emigdio/Tehachapi (northern schists)

The Rand schist of the Rand Mountains crops out in the core of a Cenozoic anticlinorium beneath an overlying sequence of Late Cretaceous diorite and pre-batholithic framework rocks along the mylonitic Rand fault (Postlethwaite and Jacobson 1987; Silver et al. 1995; Chapman et al. 2017a). During underthrusting, the Rand schist developed an inverted metamorphic gradient ranging from transitional greenschist–blueschist facies at deep levels (~3 km beneath the Rand fault) to transitional greenschist–amphibolite facies at relatively shallow levels (Jacobson 1995).

Schist exposed in the San Emigdio and Tehachapi Mountains resides beneath a series of Early to mid- Cretaceous deep-level plutonic rocks and associated pre-Cretaceous framework metamorphic rocks (Saleeby

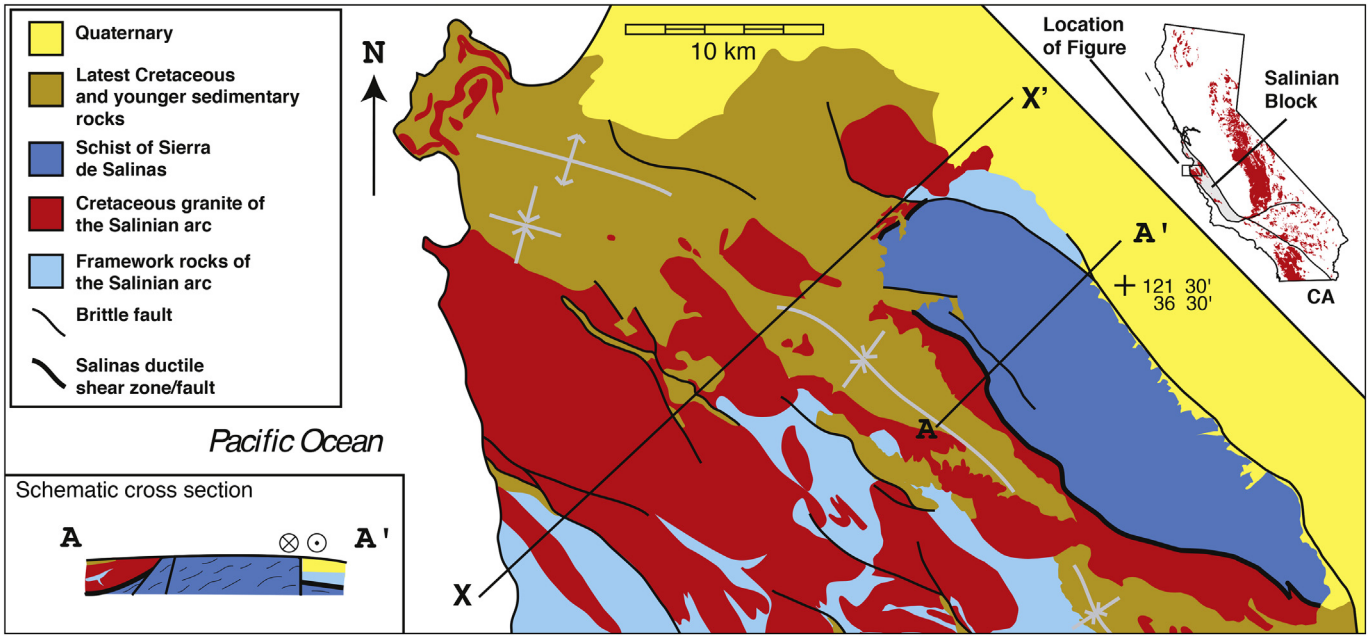

Fig. 6. Simplified geologic map of coastal central California south of Monterey Bay, showing the basement and cover units of the Salinian arc, the schist of the Sierra de Salinas, and recent sedimentary cover (modified after Ducea et al. 2007). (top right) Map showing the distribution of arc-related rocks in California. (bottom left) Cross-section A–A' depicts the structural relationships between the upper plate Salinian arc and the underlying schist. X-X' is a line along which the schematic cross sections in Fig. 7 (one for the late Cretaceous configuration and one modern) were drawn.

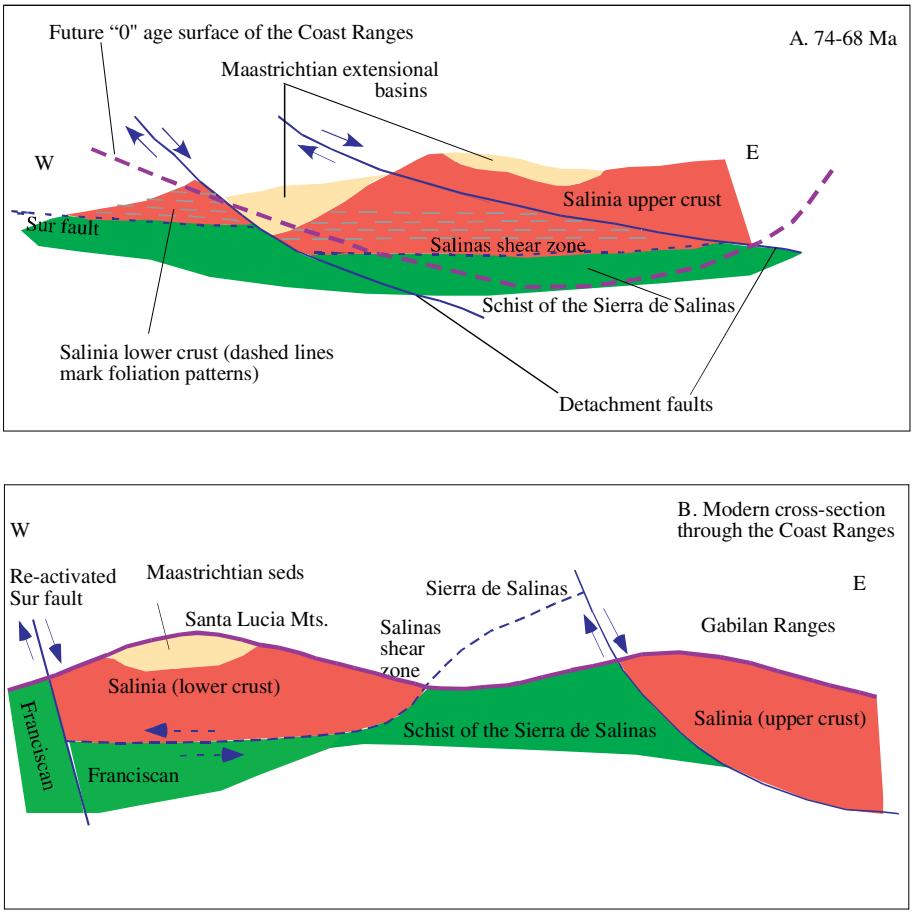

Fig. 7. Schematic W-E cross sections through the Salinia-Sierra de Salinas region: A: above, depicted immediately after underplating and during the early extension that exposed the section in the latest Cretaceous. The panel below, B, shows the geologic relationships at present day. The schist of the Sierra de Salinas is geochemically equivalent to the Franciscan formation. The approximate location of these cross sections are shown in Fig. 6 as line X-X'.

et al. 2007; Chapman et al. 2010) along a locally ductile to brittle low-angle detachment fault system that probably correlates with the type Rand fault exposed in the Rand Mountains (Postlethwaite and Jacobson 1987; Chapman et al. 2010). These schist exposures are the oldest of the schist outcrop belt, with depositional ages in the ca. 95–90 Ma range.

4.1.3. Pelona/Orocopia (southern schists)

Like the schist of Sierra de Salinas, the Pelona schist resides in the western wall of the San Andreas fault and hence is part of the SCA. All large Pelona schist exposures exhibit an inverted range in metamorphic grade from greenschist to upper amphibolite facies and are tectonically overlain by similar suites of Proterozoic gneiss and Mesozoic plutonic rocks along mylonitic shear zones (Haxel and Dillon 1978; Graham and Powell 1984; Kellogg and Miggins 2002). The Vincent fault – a ~1 km mylonite zone separating footwall Pelona schist from hanging wall Proterozoic and Mesozoic granitic rocks and gneisses – is noteworthy as it is one of few schist-upper plate contact zones that is not completely overprinted by extensional fabrics and preserves burial-related fabrics (Ehlig 1981; Jacobson 1983, 1997).

The Orocopia schist outcrop belt occupies a far inboard position, extending > 200 km inboard from the San Andreas fault (Haxel and Dillon 1978; Oyarzabal et al. 1997; Haxel et al. 2002, 2015; Grove et al. 2003a; Jacobson et al. 2007; Fig. 4). Exposures of the Orocopia schist contain peak metamorphic assemblages suggesting equilibration under greenschist to upper amphibolite facies conditions – similar to those preserved throughout the entire schist outcrop belt. All but one (Cemetery Ridge) exposure of Orocopia schist are tectonically overlain by several plates of Proterozoic and Mesozoic gneiss and granitic rocks along early to middle Cenozoic shear zones (e.g. Haxel et al. 2002; Jacobson et al. 2007; Strickland et al. 2018). The Cemetery Ridge exposure body crops out as a metamorphic pendant within an undated, but most likely middle Cenozoic (ca. 21–24 Ma) leucogranite stock (Spencer et al. 1995; Haxel et al. 2002, 2015; Jacobson et al. 2015).

4.1.4. Southernmost California and Baja California, Mexico

Though the Catalina schist currently resides within the southern California borderland, outboard of Pelona- and Orocopia-type schists, such materials formed via underthrusting beneath the northern Peninsular Ranges batholith before being rotated clockwise and translated northward to their current position (Wright 1991; Crouch and Suppe 1993; Bohannon and Geist 1998; Ingersoll and Rumelhart 1999). The Catalina schist is a series of tectonic slices, ranging from an amphibolite facies unit at the top to blueschist grade assemblages at the structural base (Grove et al. 2008).

Like the Pelona-Orocopia-Rand and related schists, the Catalina schist exhibits down-section younging, though the timing and timescales of accretion required to produce these trends are significantly different. For example, outboard-inboard age trends in the Pelona-Orocopia-Rand schist suggest that these materials were underplated in Late Cretaceous-Early Cenozoic time, over timescales of ~10 Myr or less (Grove et al. 2003a; Jacobson et al. 2011; Chapman 2017). In contrast, assembly of the Catalina schist occurred earlier (Early to Late Cretaceous, 115–105 Ma) and contains a record of over 25 Myr of underplating (Grove et al. 2008). The wide range of ages and metamorphic grades exhibited by the Catalina schist led Grove et al. (2008) to infer that these materials formed via forearc thrusting beneath the Peninsular Ranges batholith (facilitating early amphibolite facies metamorphism) and later subduction accretion of trench materials beneath previously emplaced forearc assemblages. The mechanism(s) by which these processes occurred are not well understood, but possibly involved lateral expansion due to emplacement of the Peninsular Ranges batholith, leading to forearc thrusting, followed by shallowing of the Laramide slab, underplating of mid-to-Late Cretaceous materials.

Preliminary work by Dektar and Chapman (2018) suggests that blueschist facies subduction assemblages of the Western Baja terrane, exposed on Isla Cedros (Fig. 4) and Islas San Benito outboard of the central domain of the Peninsular Ranges, were assembled in Laramide time, from ca. 95–85 Ma – much later than previously suggested (e.g. Baldwin and Harrison 1989) and postdate assembly of the Catalina schist.

4.2. Cascades core

Sauer et al. (2017) provide an excellent overview of the history of magmatism and sediment incorporation in the North Cascades Range, which is another Segment of the Cretaceous subduction-related magmatic arc found in most of the North America Cordillera. The Swakane and Skagit gneisses represent two important packages of supracrustal material situated at the deepest exposed levels of the North Cascades core. While these materials each experienced upper amphibolite facies metamorphism, it should be noted that the Swakane Gneiss is dominated by quartz-rich metasediments whereas the predominantly feldspathic Skagit Gneiss consists of < 10% metasedimentary units. Detrital zircon age and Hf isotope relations suggest that Swakane and Skagit both represent forearc materials and are inferred to have been emplaced beneath the North Cascades core in Late Cretaceous time (Matzel et al. 2004; Sauer et al. 2017; Sauer et al. 2018).

4.3. Central gneiss complex

Pearson et al. (2017) reported that some metasedimentary rocks of the Central Gneiss Complex of British Columbia and SE Alaska (Rusmore et al. 2005), presumably representing the deepest parts of this Paleogene-Eocene metamorphic gneissic complex are young (late Mesozoic or even early Cenozoic) sediments under-thrusted beneath the Coast Mountains. Detrital U—Pb age distribution of two critical areas in the Central Gneiss complex (Kwinitza and Kemano) comprises ages from 200 to 65 Ma corresponding to various magmatic events of the Coast Mountains Batholith (Gehrels et al. 2009; Girardi et al. 2012). Garnet Sm—Nd metamorphic ages from Kwinitza are 56 ± 5 Ma, consistent with U—Pb metamorphic ages on some zircon rims. The peak metamorphic pressures on garnet-bearing assemblages at Kwinitza was 9 kbar (Pearson et al. 2017 and references therein). The Kemano rocks were not investigated quantitative thermpbarometry. Metsedimentary rocks that make up some of the gnesises from Kwinitza and Kemano were formed not before 65 Ma and were buried under the main part of the Coast Mountains Batholith and metamorphosed by 56 ± 7 Ma. The age pattern is similar to other underplated metasediments in the western Cordillera implying rapid burial and metamorphism (33 km in ~ 10 My or less) Pearson et al. (2017). The relative scarcity of geologic context in that region (which is highly vegetated) makes it difficult to assess the relationships between the central Gneiss complex, which is a gigantic metamorphic core complex exposed in the core of the Coast Mountains of British Columbia and SE Alaska (Rusmore et al. 2005) and these isolated deep seated exposures. For example, the rocks at Kwinitsa, which have been studied in great detail because of their exposure (in a large quarry) and which are known to represent some of the deepest rocks regionally, may be separated from the main body of batholithic rocks and the Central Gneiss Complex by a thrust fault but such a feature has not been mapped given the terrain.

4.4. Chugach-prince william terrane

Outboard and NW of the Central Gneiss complex resides the Chugach-Prince William terrane (southern Alaska), one of the largest (~2200 km along strike) accretionary complexes in the world (Garver and Davidson 2015; Davidson and Garver 2017). It should be noted that the scale of this complex and accessibility challenges have hindered our understanding of these rocks and first-order discoveries (e.g., the recognition of numerous structural breaks within the terrane) are still being made. Detrital zircon U—Pb geochronology of turbidites from the Chugach-Prince William terrane in the vicinity of Prince William Sound

reveals that these rocks: 1) were largely sourced from the Coast Mountains Batholith and 2) young structurally downward, with maximum depositional ages decreasing from Late Cretaceous in the inboard Chugach terrane to early Eocene in the outboard Prince William terrane (Dusel-Bacon et al. 1993; Kochelek et al. 2011; Amato et al. 2013; Garver and Davidson 2015; Davidson and Garver 2017). Shortly following deposition, the Chugach-Prince William terrane was intruded by Paleocene-Eocene Kula-Farallon slab window-related plutons (the Sanak-Baranof belt; Bradley et al. 2003; Haeussler et al. 2003), resulting in local overprinting of the low-grade (generally prehnite-pumpellyite facies) Chugach-Prince William terrane by higher-grade (amphibolite facies) assemblages. These relations suggest that the Chugach-Prince William terrane was deposited, emplaced beneath the Coast Mountains Batholith and its Wrangellia Composite terrane framework, and invaded by slab window plutons – all in a very narrow timeframe (locally < 1 Myr).

Debate exists regarding whether portions of the Chugach-Prince William terrane originated near its current location (e.g., Butler et al. 2001) or thousands of kilometers to the south (possibly outboard of the Pelona-Orocopia-Rand schist outcrop belt, e.g., Garver and Davidson 2015, who invoke Laramide shallow angle subduction as the burial mechanism for the Chugach-Prince William terrane). Regardless of the origin of the Chugach-Prince William terrane, its structural position beneath the Coast Mountains Batholith plus spatial variations in depositional age indicate that these materials qualify as a Cordilleran underplated complex.

5. Margin evolution during tectonic underplating

Eroding subduction margins require that the trench migrates inboard to the upper plate, leaving older arcs progressively closer to the trench (Scholl and von Huene 2007). While there is little work in the literature to document the rates of such migration in the geologic record globally, the two end member forms of migration can be either catastrophic or pseudo-steady state.

We define catastrophic/sudden trench migration episodes as time periods when the trench moves inboard by 100 s of km; this is equivalent in scale to out of sequence thrusting in collisional belts and led to underplating of all of the western Cordilleran examples above. Magmatic arcs step accordingly inboard during the initiation of such events, which are taking place during ultra-shallow subduction periods. Their likely trigger is buoyancy of the downgoing plate – such as the arrival of a subductable oceanic plateau. In western North America, the initiation of ultra-shallow subduction on the early Laramide orogen (Saleeby 2003) was triggered by the arrival and subduction of the Hess-Shatsky conjugate oceanic plateau (Fig. 8, Liu et al. 2010; Li et al. 2011, Quinn et al. 2018).

Smaller inboard steps of the trench (~10s of km) will give a pseudo-steady state appearance to the process. Most modern examples of forearc underplating (such as the Cascadia example presented above) represent step backs of that magnitude. This type of eroding margin will also lead to migration of the arc inboard but in much smaller increments, compared to catastrophic trench migration. Typical "steady-state" migration occurs at rates of 1–5 mm/yr, as it can be inferred from the age of old arcs in contact with the trench today given the average distance of arcs from trenches in modern subduction systems (Ducea et al. 2015).

Clearly, not all the sediment transported downward with the subducting plate at eroding margins needs to return to the upper plate by underplating. A yet to be quantified fraction can be subducted deep into the mantle and some may return to the upper plate by arc magmatism. But as it has been pointed out by classic papers on subduction erosion (von Huene and Scholl, 1991, Clift and Vannuchi, 2004, 2009), the magnitude of sediment eroded away at modern margins is staggering. At rates of subduction erosion similar to today, much of the continental crust would be consumed into the mantle over a 1–2 Ga period. A large fraction of subducted accretionary wedge sediment must somehow be transferred back to the upper plate and we propose here that underplating is the most important candidate mechanism for that, while relamination or other form of melt transport are of secondary importance at least until tests of the mechanism or future relevant discoveries in the geologic record may inform us otherwise.

6. Underplating from the forearc or backarc side

One critical question addressed in virtually all papers documenting underplating in western North America is whether metasedimentary materials now found structurally under the core of the orogen were

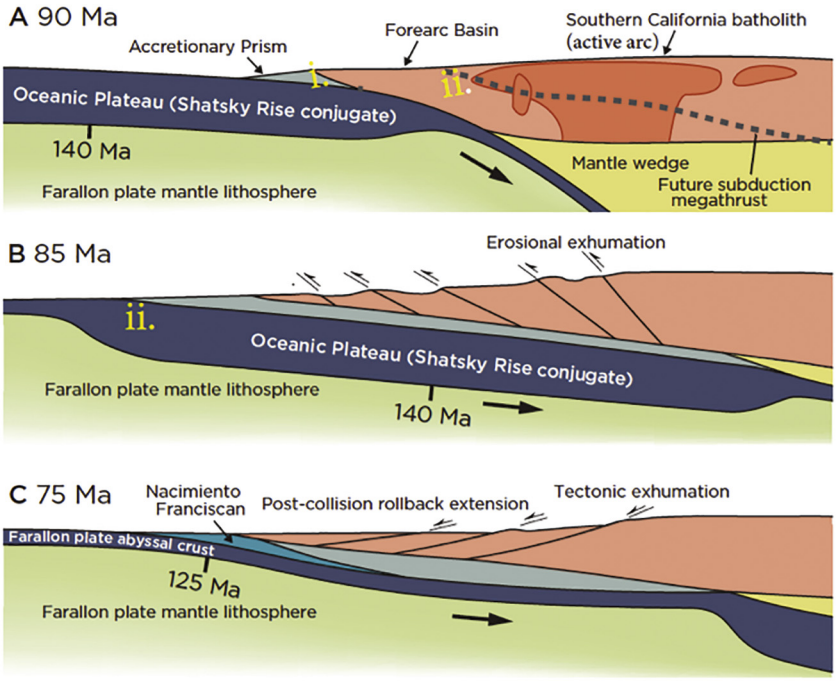

Fig. 8. Schematic cross sections through the central California geology showing the modifications to the subduction margins brought on by the arrival of the Shatsky Ridge conjugate plateau, which is believed to have triggered the ultra-shallow event represented by the Laramide orogeny (diagrams modified after Quinn et al. 2018). Note also that the plate margin retreated with the initiation of shallow subduction (former location of the trench on the upper plate, point "i" was subducted and the new location of the trench touching the upper plate became point "ii", approximately 150–180 km inboard. Consequently, much of the former accretionary wedge, forearc and even parts of the California arc were underplated.

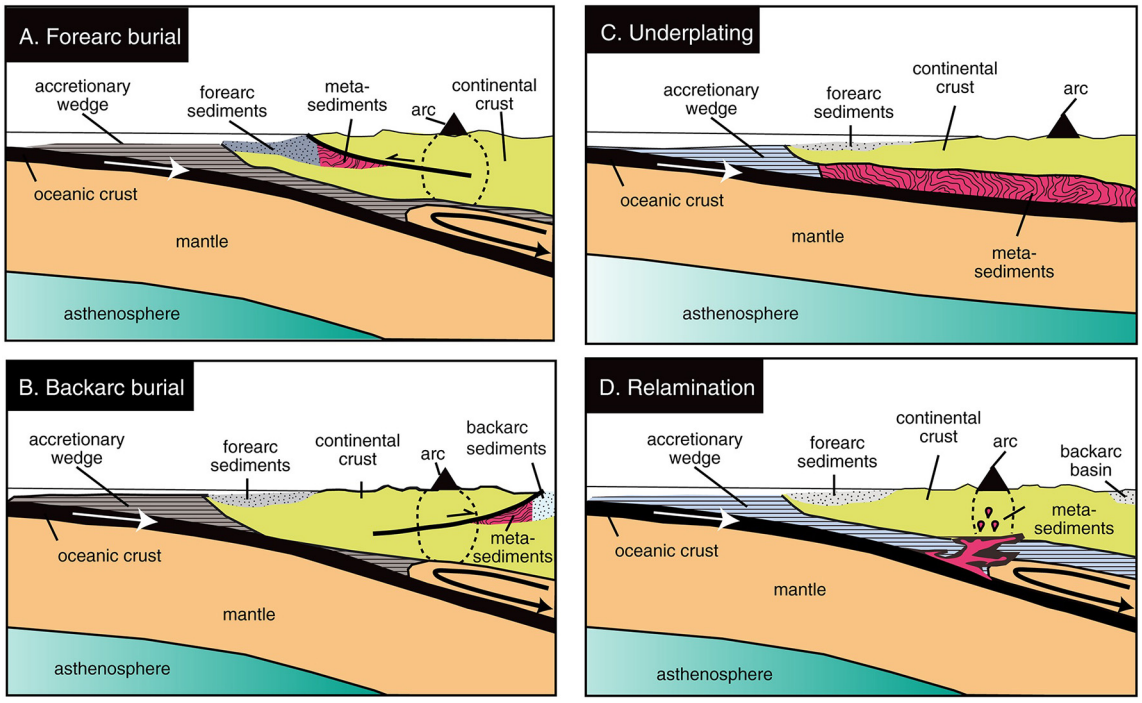

Fig. 9. Plausible destinations of metasedimentary material during underthursting beneath a Cordilleran magmatic arc: (A) forearc thrusting under the arc along reverse faults, (B) accretionary wedge underthursting along the main subduction plane, (C) burial and thrusting from the backarc side, and (D) relamination of subducted sedimentary materials (solid state or partially molten). (from Gordon et al. 2017, Sauer et al. 2017, modified after an original figure in Haxel et al. 2002).

delivered from the forearc or backarc side (Fig. 9). For some. Forearc underthrusting includes two subtypes- accretionary wedge and forearc proper (Gordon et al. 2017). A more controversial mechanism not involving shortening and thrust faults and referred to as relamination is yet another mechanism that in theory can attach metasediments to the bottom of arc sections in Cordilleran orogens (Fig. 9d). This will be discussed briefly in a separate section below.

Retroarc thrusting is inferred based on the geochemistry and isotopic compositon of arc magmas to have played a significant role in triggering high flux events in Cordilleran magmatism (Ducea 2001; DeCelles et al. 2009; Ducea et al. 2015). Could the exposed sections described in this paper be the physical evidence for retroarc thrusting? From a purely geologic/structural standpoint, the modern-day structures are telling us little about their original vergence, as they were rotated and often reactivated as normal faults. The forearc versus backarc origin may be better answered by deciphering the provenance of the metasedimentary rocks and information regarding the speed of burial.

Provenance is easiest assessed using U—Pb ages on detrital zircons (Gehrels 2014) as it has been performed on various North American examples described above (e.g. Grove et al. 2003a). Rocks originating in the forearc or trench will predominantly have zircons originated in the nearby magmatic arc (predominantly Jurassic-Cretaceous ages in the SCA for example), whereas backarc source sediments are expected to have a mix of arc-related ages and older continental ages reflecting the origin and evolution of that particular backarc segment. In most cases, the arc itself is a significant topographic barrier for most of the lifecycle of a subducting margin and sedimentary pathways from behind the arc and into the forearc are limited. All examples reviewed in this paper are more consistent with a forearc/trench origin as they are dominated by the presence of arc-aged zircons (Barth et al. 2003; Jacobson et al. 2011; Pearson et al. 2017; Sauer et al. 2017).

Speed of burial is the time difference between deposition and peak metamorphism, and is sometimes difficult to estimate because metamorphic rocks that achieved amphibolite grade do not preserve any fossils and determining the age of deposition is not trivial. However, many of the underplated rocks contain detrital zircon grains of near depositional age derived from proximal arcs (Ducea et al. 2009). The maximum depositional age constrained by the youngest zircon peak is therefore commonly used in determining burial time. Peak metamorphic time is constrained either by garnet-whole rock geochronology (Ducea et al. 2003b), by zircon U—Pb ages of dikes cross-cutting metamorphic fabric or metamorphic rims on detrital cores (Matzel et al. 2004; Chapman et al. 2013; Sauer et al. 2017), via Ar—Ar amphibole and/or mica cooling ages (Grove et al. 2003a; Jacobson et al. 2011); or by monazite U-Th/Pb geochronology (not applied, so far in the examples discussed herein). The small difference between timing of deposition and metamorphism (3–5 My) where this was assessed (Maztel et al., 2004; Ducea et al. 2009, Pearson et al. 2017) all suggest that the carrier was the main subduction megathrust and the likely origin of the lower plate metasediments is the accretionary wedge, although forearc underplating could also be responsible (Matzel et al. 2004). These speeds of burial (30 km/My, or 3 cm/yr), are typical of rates found at plate margins, whereas orogenic thrust faults (whether developed in a forearc or retroarc environment, as well as in typical collisional belts) are characterized by rates of movement about an order of magnitiude lower (several millimeters per year, DeCelles et al. 2002). The speed of burial argument is as important as any in deciphering underplating the rock record.

An additional key relationship observed in most underplated terranes is the presence of up-section increases in both age and metamorphic grade, which are opposite the trends typically found in the crust. These observations are readily explained by sequential underplating of progressively younger material beneath an upper plate that is losing heat to the material underplated beneath it. Shear heating is unlikely to have contributed much to observed lower plate heating, as underplated materials are often too weak to sustain the stresses required to promote significant shear heating (Kidder and Ducea 2006; Kidder et al. 2013). It should be noted that down-section younging has not been reported in any individual window of the Pelona-Orocopia-Rand schist outcrop belt, though regional scale age trends are interpreted by some to be the product of inboard/down-section younging

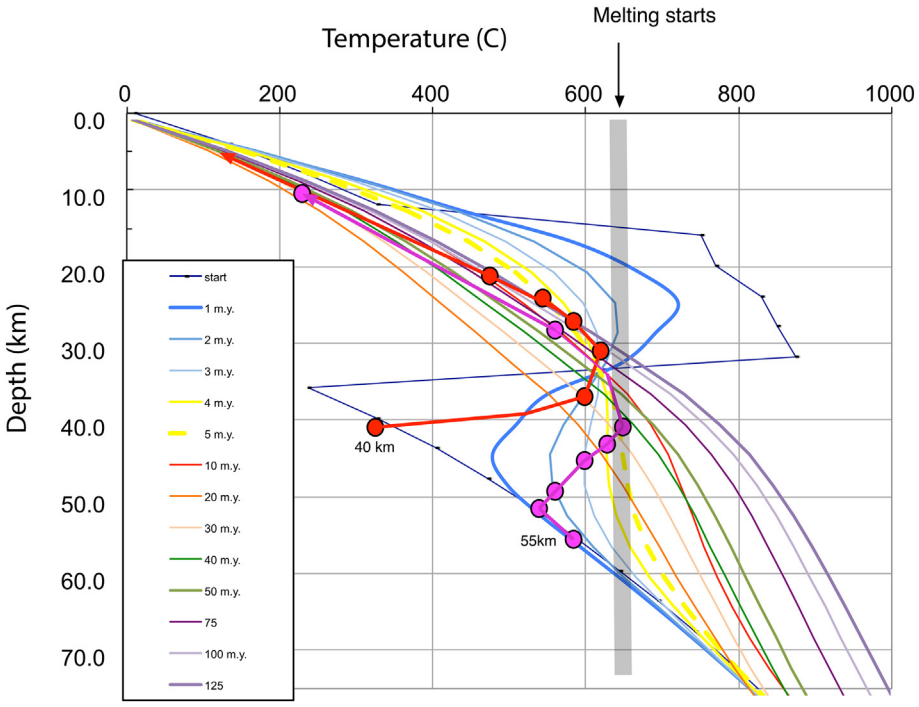

Fig. 10. 1-D thermal modeling (time versus depth) showing the effects of thrusting a cold sheet under a magmatic arc section over time. Thrusting is taken to be instantaneously and thermal gradients are shown for various time intervals after underplating (see colour coded panel to the left). The path of two material points from the lower plate, one starting at 40 and the other at 55 km are shown corresponding to unroofing rates of 1 mm/yr. The slower the unroofing rate and the deeper the point of origin, the more likely it is for the lower plate to exceed its solidus (shown in this figure as a generic temperature range for wet melting of granites). Clearly, with inverted temperatures still preserved in some of the SCA exposures, unroofing must have been significantly faster than 1 mm/yr and the likelihood of extensive partial melting is low. The minimum temperature for partial melting (wet granite solidus) is indicated with a thick grey line.

(e.g., Chapman 2017).

Lithologies other than metasedimentary present in these regional examples are various mafic to ultramafic lithologies presumably representing various fragments of the Pacific plate that are caught in the accretionary assemblage. < 5% of the schist of the Sierra de Salinas contains serpentinites and various amphibole-bearing gabbroic rocks sensu-*lato* (Diblee, 1972; Ross 1976), and while that number varies from exposure to exposure in the SCA, it never exceeds some 10% of the exposed schists. Similarly, the Cascades core exposures, those in the Central Gneiss Complex, the Condrey Mountain schist, and Catalina/Cedros Island contain isolated exposures of serpentinites and related mafic material. They do not have an impact on the strength of these underplated sections but their presence can be useful in testing forearc versus backarc origins for underplated sections. While mafic materials can be found in backarc basins, they may not be oceanic as one expects from mafic materials originating in the forearc or accretionary wedge. Accretionary wedge mafic-ultramafic rocks are expected to have either MORB-like geochemical/isotopic characteristics or seawater-altered MORB compositions. In contrast, most back arc-related mafic magmas formed in the North and South American Cordillera have isotopic characteristics suggestive of old continental crust and mantle lithosphere as one of the melt sources (Chapman et al., 2014; Chapman et al. 2017b). Little work has been done on the mafic/ultramafic components in the SCA or elsewhere. The dominantly mafic magmatic and peridotitic (although highly altered) exposure at Cemetery Ridge (Haxel et al. 2015) is particularly attractive for such a study in the future.

7. Relamination?

A relatively recent proposal suggested that metasedimentary assembages found structurally under magmatic arcs may have been emplaced there convectively as a result of a process referred to as "relamination (Behn et al. 2011) and subsequent publications). Relamination requires that subduction complex-related sediments are buried to significant depths in the mantle at the top of the slab and subsequently rise diapirically, penetrate through the mantle wedge (mix with mantle wedge assemblages along the way) and ultimately get attached to the bottom of the upper plate.

This is quite different from the thrust-fault style deformation at subduction megathrust discussed above and requires a different, larger pressure-temperature-time path loop for the metasediments; peak metamorphic depths should be in the range of 100 km or more followed by adiabatic decompression. Moreover, one would predict some peridotitic mantle assemblages to be mixed in the relaminated material. To our knowledge, nowhere has ultrahigh pressure metamorphism been observed in underplated subduction complexes, and the Cordilleran examples above do not particularly contain significant amounts of mantle wedge assemblages mixed with the metasedimentary rocks (and if mafic-ultramafic rocks do exist, they are more likely to represent scrapped off pieces of the downgoing slab). The exception is the Cemetery Ridge exposure – the easternmost exposure of the Southern California allochthon- does contain suprasubduction related mantle peridotite (Haxel et al. 2015) but they are interpreted to represent mantle lithosphere which separated upper plate crust from underplated sediments at this far inland location. There are no data to suggest that the predominantly metaclastic metasediments exposed at Cemetery Ridge underwent ultrahigh or near ultrahigh pressure metamorphism (Haxel et al. 2015).

Future geologic tests may provide more in-depth tests of the relamination hypothesis. So far however, the existing body of data for the underplated assemblages of western North America suggest that thrusting during shallow and ultra-shallow subduction was the mechanism responsible for burying subduction complexes far under the forearc and magmatic arc of the subduction system. The continuity of inferred sedimentary units from the trench to forearc in seismic data from Cascadia and Mexico presented here also indicate that at least in those cases, the pathway to underplating is a shallow one and not involve a loop through the mantle wedge.

8. Thermal evolution and metamorphism

Fig. 10 shows temperature depth time patterns for a material point initially located at 40 km beneath the surface following underplating (red circle), and another one at 55 km beneath the surface (purple circle). These patterns assume an exhumation rate of 3 mm per year, which was determined for the schist of the Sierra de Salinas (Ducea et al. 2009) and is probably typical for the entire fast exhuming southern California allochthon during the Late Cretaceous. The

underlying thermal gradients were determined using a 1-D thermal model (Turcotte and Schubert 2014) in which an instantaneous low plate was thrust under a hot upper plate (continental crust). The upper plate has typical arc magmatic thermal gradients with a hot zone of > 750 °C (mafic magmatic additions) in its lower part. The contact was placed at 35 km beneath the surface, similar to the field examples given above. A z-shaped bending of the thermal gradients at the start of the model gradually relaxes over time to where a negative thermal gradient disappears from the top of the underthrusted slab after several million years. Thermal gradients are shown at 1 million year intervals for the first 5 million years and progressively greater temporal spacing afterwards. Fig. 10 shows how unlikely it is that the underplated materials will undergo partial melting. A minimum melting temperature of around 625-650 °C for granitic materials is shown for comparison- see also discussion below regarding melting.

However, one can also notice that a significant amount of heating takes place in the underplated slab even within the relatively short window of thermal relaxation imposed by the 3 mm/yr exhumation rate. Obviously higher temperatures would be attained if lower rates of exhumation would be applied. Nevertheless, the underplated sediment would be definitely subjected to Barrovian metamorphism in the 400–600 °C range. Therefore the overall high grade Barrovian, garnet grade, aspect of these rocks is rather expected by the simplest of predictions; these rocks are not high pressure/low temperature rocks, although they may have started that way and despite the fact that they are fundamentally "subduction complexes". In other words, subduction complexes are likely to develop amphibolite and locally transitional granulite facies metamorphism in situations in which they are removed from the fast burial (and exhumation) typical for the downgoing plate. Consequently, many subduction complexes attached (underplated) to the upper plate may be missed in the geologic record if one expects subduction complexes to be metamorphosed under high pressure –low temperature conditions.

9. Melting

Do underplated sediments melt? The PTt paths outlined in Fig. 10 show that if exhumation is taking place at a rate of 3 mm/yr or faster, there is very little thermal relaxation time to reach minimum melting temperatures for underplated rocks, although clearly they are overall fusible materials (high water content and first cycle, upper crust rocks). Thermal relaxation times of 10- my or more are needed to bring quartzo-feldspathic sediments taken to lower crustal conditions above standard wet-granite solidi (Johnson et al. 2008), which correspond to temperatures in excess of 650 °C, at 1–1.3 GPa pressures typical for the regional examples given above.

The western North American Cordilleran examples excepting the Cascade Core examples experienced little to no partial melting, partly because they were exhumed relatively quickly in the forearc position they resided (see "Extensional Collapse" below). However, when the competing effects of thermal relaxation (heating) and extensional unroofing (cooling) are in favor of the first (low unroofing rates, < 0.5 mm/yr) typical metasedimentary terrigenous trench-derived sediments can clearly undergo partial melting at relatively low temperature, if water is present. Muscovite-dehydration melting is probably the most likely melting reaction expected to take place in such a situation.

We conducted a series of partial melting forward models using the Rhyolite MELTS program in order to determine the most likely melt compositions to be extracted in the 1 to 2 GPa and 600–800 °C pressure temperature window. The starting material is an average composition of the lower structural part of the schist of the Sierra de Salinas (Kidder and Ducea 2006), assumed to contain 1% H_2O. Melting started at around 670 °C in these models. Silica concentrations in partial melts are shown in Fig. 11 as a function of temperature (and pressure).

The purpose of showing these results is primarily to illustrate general trends and not to investigate them in detail. All melt compositions

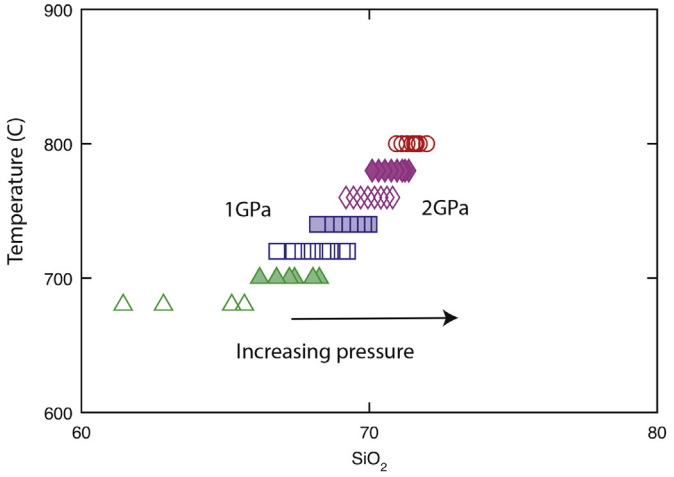

Fig. 11. Predicted silica concentration of partial melts formed by a starting material averaging the schist of the Sierra de Salinas (Ducea and Kidder unpublished data) from 1 to 2 GPa and 670–800 °C (using Rhyolite MELTS). The diversity of compositions plotted here for various PT conditions are in detail not so relevant; overall they show that the predicted melts will be aluminous and silicic, S-type granites.

are silicic (with an average SiO_2 = 70%) and are peraluminous, S-type granitoids, with high alkali content, as one might expect as the melting product of a metasedimentary assemblage. Only at the lowest temperature-pressure domain investigated here, the melts are not per-aluminous and have predicted major elemental chemistries more similar to the main Cordilleran batholiths; however, in that PT window, melt productivity is insignificant. Silica increases with higher temperatures and pressures (Fig. 11). Consequently the PT domain having the greatest chance to partial melt will produce highest silica rhyolites.

These results have some important implications for arc magmatism. Episodes of tectonic underplating can take place repeatedly in long-lived Cordilleran environments. While obviously tectonic underplating beneath an arc shuts down the arc at that location temporarily (and moves it inboard), as demonstrated by the thermal model presented above, subsequent steepening of the slab or other mechanisms can bring the arc location back to where underplated sediments reside. The presence of S-type granitoids in the magmatic archive of a long-lived Andean arc signifies partial melting of deeply emplaced metasedimentary rocks (Ducea et al. 2015). Production of S-type granitoids early in the lifetime of a magmatic arc can be the result of melting upper plate passive margin sediments (Wetmore and Ducea 2011). On the other hand, for those S-type melts that form tens of millions of years later than the arc initiation (Miller et al. 1996; Chapman et al. 2013; Van Buer et al. 2016), they probably represent partial melts of meta-sediments that were emplaced in the mid-lower crust during the subduction process, or otherwise those melts would have been extracted into the arc during the initial stages of magmatism.

10. Fossil subduction megathrusts

Ultra-shallow subduction leading to underplating of upper crustal sediments below the upper plates requires that temporary subduction interfaces (megathrusts separating the subducting lower plate from the upper plate) remain preserved in the geologic record after underplating (Ducea et al. 2007). Indeed, burial-related microstructures are reported in California from the Salinas shear zone, the Rand fault in the San Emigdio Mountains, and the Vincent fault in the San Gabriel Mountains (Fig. 5; Jacobson 1983; Kidder and Ducea 2006; Ducea et al. 2007; Chapman et al. 2010; Xia and Platt 2017). In most other places of the southern California allochthon, the subduction interfaces were reactivated as normal faults (see Fig. 6 for some parts of the Salinian

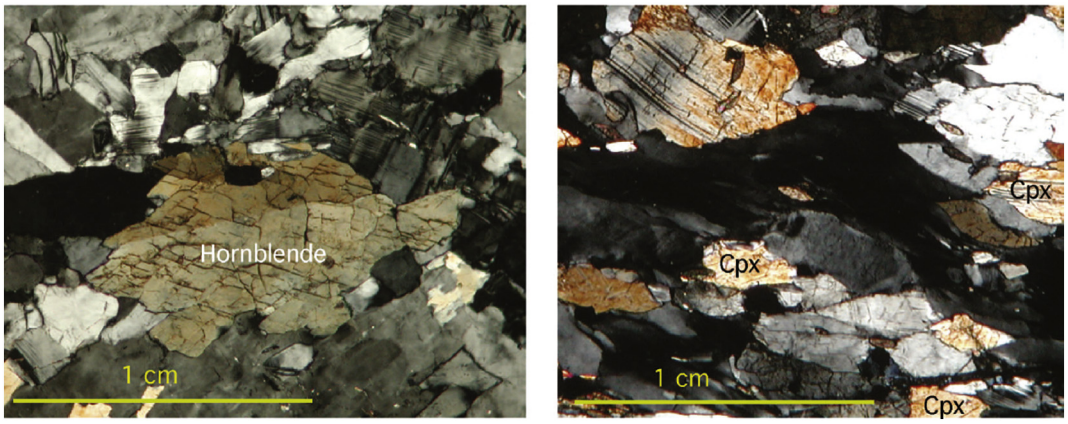

Fig. 12. Microphotographs from a single thin section (crossed polars) within the Salinas shear zone showing association of granulite facies metamorphism with deformation. (right). A highly deformed band from the shear zone. The yellow crystals are clinopyroxene (labeled 'cpx'). Deformation twins in large grain can be seen in the upper left. Dynamically recrystallized quartz dominates this part of the slide. (left) A less deformed band where hornblende is preserved (from Ducea et al. 2007). (For interpretation of the references to colour in this figure legend, the reader is referred to the web version of this article.)

exposures) and field relationships reflect that extensional phase that juxtaposed the lower and upper plates of the system.

The Salinas shear zone (Ducea et al. 2007) is a particularly insightful area because it reveals two remarkable features of the subduction megathrust: the ductile shear zone, which itself is not much thicker than a few hundred meters reveals hotter and drier granulite conditions for both the upper and the lower plates. Thermometry in the shear zone reveals temperatures that are at least 75–100 °C hotter than the upper plate (the lower plate is colder still) (Ducea et al. 2007). Fig. 12 comprises two microphotographs from the shear zone showing the features observed at the core of the ductile deformation zone. Pyroxene grows at the expense of amphibole, essentially providing a transition from amphibolite to granulite facies rocks in the shear zone. This observation is inconsistent with the idea that such mega-faults are lubricated and are subject to really low friction between the two blocks and consequently undergo insignificant shear heating (Kidder et al. 2013). Instead, we see quite the opposite, the shear zone has lost water and underwent dehydration reactions stabilizing pyroxenes at the expense of amphiboles and maybe lost some partial melt as well. If the shear zone acted as a sealant for fluids, granulite facies metamorphism would not have developed at paleo-depths of 30–35 km. Similarly, garnet grains from upper structural levels of the San Emigdio schist exhibit fractures filled with hydrous minerals, suggesting that prograde metamorphic dewatering accompanied transient high strain rate events within this schist body (Chapman et al. 2011). Geophysicists have identified episodic tremor and slip along shallow subduction zones worldwide at depths similar to the paleo-exposure levels of the Salinas shear zone [e.g., Melbourne and Webb 2003]. Tremors common during 'slow earthquake' events are interpreted by some researchers to represent fluid bursts in or out of the fault zone. Tremors occurring today beneath the Cascadia subduction zone may represent dewatering during ductile slip along the megathrust at depths of some 30–50 km (Melborne and Webb, 2003).

The observations on the Salinas shear zone are certainly preliminary and require further study since these are extremely rare situations in which fossil subduction megathrusts are exposed in the geologic record. Structures like the Salinas shear zone can link many of the geophysical observations from modern settings to large-scale geologic processes, such as the development of granulite facies metamorphism, dewatering, and structural slip as reported here, and thus advance our understanding of physical processes along subduction faults.

11. Extensional collapse

Extensional collapse is a key element of most Cordilleran and other types of orogens which leads to crustal thinning and exposure of deeper crustal rocks. The SCA collapsed extensionally soon after the underplating of the schists, during the Late Cretaceous (e.g. Kidder and Ducea 2006; Barbeau et al. 2005). Indeed, most faults exposing the contact between upper plate (North American continental crust) and the lower plate (the subduction complexes) are normal faults representing reactivations of earlier thrust faults. Of all SCA examples, Salinia/schist of the Sierra de Salina is perhaps the best preserved natural laboratory for extension as well. It clearly underwent major extension (Fig. 7) soon after the emplacement of the Sierra de Salinas schist in the latest Cretaceous. Yet, the original thrust contact was not reactivated, at least where it is currently exposed. It took < 5 My from the deep crustal arc

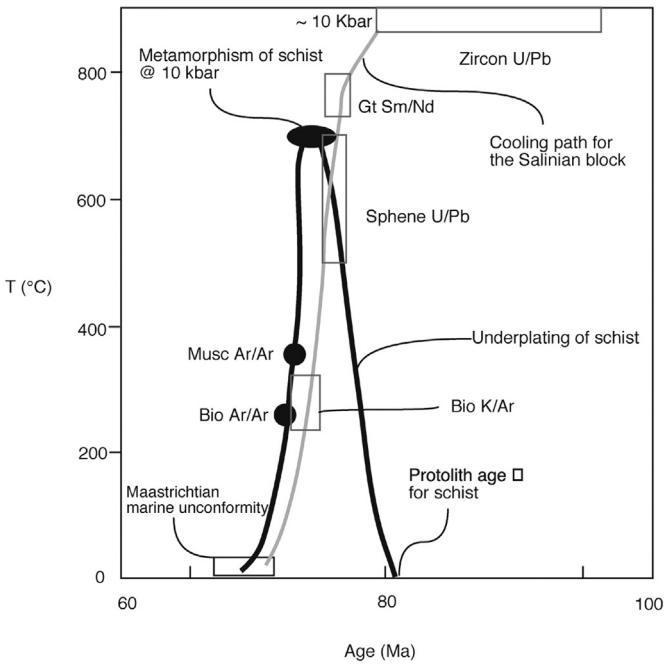

Fig. 13. Temperature-age diagram for the upper (grey line) and lower (dark line) plates of the Salinia-schist of the Sierra de Salinas example. The schist formed at about 80 Ma and was quickly buried to about 1 GPa (10 kbar), whereas the upper plate was at similar pressures as a magmatic arc at 80–90 Ma. Various geo and thermo-chronometers as well as geologic constraints document that the two had a common history starting at about 77–76 Ma and underwent rapid extensional collapse as a single unit (modified after Ducea et al. 2009).

exposures of Salinia's western block to be exhumed at the surface and be covered by submarine fan deposits (Fig. 13, modified after Ducea et al. 2009; Kidder et al. 2003). Several thermochronometers measured by various researchers on the upper and lower plates of the Salinia-schist of the Salinas region as well as geologic constraints such as the age of sedimentary cover (Fig. 13) provide a compelling case that the hanging wall and footwall of this system were connected at around 76–78 Ma and underwent fast unroofing immediately after. Such rates of unroofing are only consistent with extensional collapse of the system (Ducea et al. 2009) and cannot be explained by erosional processes alone. A similar history of continental extension immediately following the episode of underplating is discernible in all SCA exposures but to a lesser extent in the gneissic exposures to the north.

Below, we speculate on the possibility that the extensional collapse of the SCA forearc could have been triggered by the predominantly quartz- and mica-rich lithologies of the schists among the underplated materials, in contrast to the plagioclase-rich nature of the lower plate rocks of the Central Gneiss region and those from the Cascades.

12. Schists or gneisses?

Some of the underplated assemblages described above are dominated by schists and others by gneissic rocks. In addition, the sequences of lower plate rocks also contain quartzite (very common) some carbonates (e.g., Kwinitza, Pearson et al. 2017; and some exposures of the Pelona-Orocopia-Rand schist, Dawson and Jacobson 1989), and some mafic/ultramafic assemblages. The relative abundance of plagioclase versus quartz in the original sedimentary assemblage is the deciding factor in the composition of the metamorphosed rocks, i.e. whether they become schists or gneisses. Subduction complexes contain a large variety of lithologies, some quartz-dominated others plagioclase-dominated, if they are derived from a nearby arc. The richer in feldspar they are, the more difficult it is to determine the sedimentary origin of a metamorphic rock, since the silica content is lower and overlaps with those of intermediate volcanic rocks. At 65% SiO_2 or less, many of the deepest rocks of the central Gneiss complex are geochemically ambiguous: they could have been forearc/trench terrigenous sediments derived from the Coast Mountains batholith or could have been volcanic sequences buried from the back arc side (Pearson et al. 2017). The same applies for the rocks of the Swakane or Skagit gneiss. Nevertheless, if the assemblage is dominated by gneissic rocks (which we refer to as “Skagit-type” underplated terrains, based on the name of the best studied example in North America), the strength of these rocks remains significant even if they are heated to over 600 °C; this aspect may be important in facilitating or hindering regional extensional collapse (see next section). Of course, the mechanisms by which forearc materials are shallowly emplaced beneath arcs (e.g., oceanic plateau subduction) tend also to drive upper plate contractile deformation, leading to a buildup of gravitational potential energy (Dewey 1988; Rey et al. 2001; Chapman et al. 2012). We simply argue here that gravitational collapse of the overthickened upper plate following for example, passage of an oceanic plateau may be accelerated by the presence of quartz-rich underplates or stalled by feldspar-rich lower plate materials.

At the other end member of the spectrum, quartz-rich schists, which are typical for the SCA, are high silica rocks that were most likely derived from sediments (referred to as Salinas-type). These rocks are dominated by quartz and white mica and have little to no strength at high temperatures (Kidder and Ducea 2006). A thick package of underplated schists is likely to make up a weak lower crust, which in turn, is prone to gravitational collapse of the upper part of the crust. This may explain why regionally, the SCA has undergone extensional collapse rather quickly after the emplacement of the schists in all of the preserved examples. If there is any merit to the speculation that more feldspar-rich materials are more likely to reside at greater depths because of their strength, those same materials are more likely to melt than quartz-richer lithologies. In other words, the richer the arc-related (and continent-related) input into the accretionary wedge, the more likely it is that these materials will melt again after underplating, if they are subject to such a process.

13. Significance to continental evolution

Is tectonic underplating significant at convergent margins over time? With a global modern average subduction angle of < 20 degrees near the trenches, one would expect the process to be significant today and by analogy to be more common in the geologic past than usually acknowledged. Underplated rocks will be subject to regular Barrovian metamorphism as described above and the fact that they are not preserved as high pressure-low temperature rocks makes them easy to overlook in the geologic record.

Trench-side underplating produces crustal inversions whereby first cycle upper crustal rocks (sediments) are being delivered into a lower crustal position. The following are consequences of underplating:

1. *A more felsic composition of the lower crust*. Tectonic underplating can account for significant amounts of metasedimentary material to occupy the lower parts of the crust, something that has been known for many Cordilleran arcs that are exposed to mid-crustal levels (Ducea et al. 2003a; Chapman et al. 2012; Chin et al. 2013). It is not clear where the sub-arc lower crustal and upper mantle assemblages disappeared to following underplating of the North American west, but some fragments of laterally displaced materials have been recognized in the continental interior, while others were likely recycled into the mantle. Hence, sub-arc underplating results in the swapping of significant volumes of mafic and ultramafic lower crust/upper mantle with upper crustal felsic sedimentary units. Tectonic underplating therefore may be a mechanism contributing to the generation of the continental crust, which appears more felsic on average (Rudnick and Gao 2014) than was previously thought to be.
2. *A lower crust that is stable with respect to foundering*. Most lower crustal arc sections are prone to delamination (Ducea 2002; Jull and Kelemen 2001) because of the accumulation of dense mafic and ultramafic magmatic arc residual rocks, particularly pyroxenites with or without amphibole and/or garnet. Episodes of tectonic underplating are replacing those types of materials with less dense metamorphic rocks that are normally not likely to founder into the asthenosphere. If the average densities of arc root assemblages at 1–2 GPa are 3.4 to 3.6 g/cm^3 at the hot zone (Annen et al. 2006) temperatures of 900 °C, the density of metamorphosed subduction complex does not exceed about 2.9 g/cm^3 even after melt extraction (see supplementary data), and are more typically around 2.8–2.9 g/cm^3. The presence of ultramafic materials in the subduction complex does not usually increase the overall density since those materials are typically serpentinized and present in minor amounts. In other words, underplating stabilizes continental crust from convective removal.
3. *A lower crust that is capable of flash melting under favorable circumstances*. The presence of first cycle sedimentary materials at great depths can trigger major S-type granite flare-ups either at a later stage in the evolution of the arc or during extension events following the demise of the subduction system.

14. Summary

Tectonic underplating of trench and forearc materials during episodes of ultra-shallow subduction and trench retreat represents a major process for adding sedimentary-dominated upper crustal masses to the lowermost crust of subduction upper plates. We reviewed geologic evidence for this process in western North America. Examples presented here represent the products of shallow subduction during the late Cretaceous and early Cenozoic. The best case studies come from

southern California where the underplated rocks are found beneath magmatic arc rocks of the cordilleran subduction system. The sharp contrast between the hot assemblages of mid- to lower -crustal batholitic assemblages in the upper plate and the relatively cold schists below made this process easily discernable at many of the southern California locations. Other locations in western North America (and beyond) are now known, but they would have been difficult to discover without the knowledge accumulated over decades from the southern California locations. The implications of this structural process to destroying and rebuilding the continental crust, its thermal state, future magmatism, and the origin of continental crust in general are significant.

Acknowledgments

Our view on tectonic underplating was influenced over the years by work done by long term collaborators Steve Kidder, Jason Saleeby, Dave Pearson and the late Bill Dickinson as well as our peers Andy Barth, Carl Jacobson, Gordon Haxel, Marty Grove, Jennifer Matzel, Bob Miller, Stacia Gordon, Cam Davidson, John Garver, and others through their significant discoveries made in this field. This manuscript was critically and constructively reviewed by Dave Scholl, editor Arturo Gomez Tuena and an anonymous reviewer. MND acknowledges support from US National Science Foundation Petrology-Geochemistry grant EAR 1524110 and the Romanian Executive Agency for Higher Education, Research, Development and Innovation Funding project PN-III-P4-ID-PCE-2016-0127. ADC received support from NSF grants EAR-PF1250070 and EAR-1524768.

References

Amato, J.M., Pavlis, T.L., Clift, P.D., Kochelek, E.J., Hecker, J.P., Worthman, C.M., Day, E.M., 2013. Architecture of the Chugach accretionary complex as revealed by detrital zircon ages and lithologic variations: evidence for Mesozoic subduction erosion in south- Central Alaska. Geol. Soc. Am. Bull. 125, 1891–1911.

Annen, C., Blundy, J.D., Sparks, R.S.J., 2006. The genesis of intermediate and silicic magmas in deep crustal hot zones. J. Petrol. 47, 505–539.

Baldwin, J., Harrison, T.M., 1989. Geochronology of blueschists from west-Central Baja California and the timing of uplift of subduction complexes. J. Geol. 97, 149–163.

Barbeau, D., Ducea, M.N., Gehrels, G.E., Saleeby, J.B., 2005. Detrital-zircon U-Pb geochronology and the origin of Salinia: Geological Society of America Bulletin. 117. pp. 466–481.

Barth, A.P., Wooden, J.L., Grove, M., Jacobson, C.E., Pedrick, J.N., 2003. U-Pb zircon geochronology of rocks in the Salinas Valley region of California: a reevaluation of the crustal structure and origin of the Salinian block. Geology 31, 517–520.

Behn, M.D., Kelemen, P.B., Hirth, G., Hacker, B.R., Massonne, H.-J., 2011. Diapirs as the source of the sediment signature in arc lavas. Nat. Geosci. 4, 641–646.

Bohannon, R.G., Geist, E.L., 1998. Upper crustal structure and Neogene tectonic development of the California continental borderland. Geol. Soc. Am. Bull. 110, 779–800.

Bradley, D.C., Kusky, T.M., Haeussler, P.J., Goldfarb, R.J., Miller, M.L., Dumoulin, J.A., Nelson, S.S., Karl, S.M., 2003. Geologic signature of early Tertiary ridge subduction in Alaska. In: Sisson, V.B., Roeske, S., Pavlis, T.L. (Eds.), Geology of a Transpressional Orogen Developed during Ridge-Trench Interaction along the North Pacific Margin. Vol. 71. Geological Society of America Special Paper, pp. 19–49.

Burg, J.P., A. Dolati, D. Bernoulli, and J. Smit, 2013, Structural style of the Makran tertiary accretionary complex in SE-Iran, 2013: in K. Al Hosani et al. (eds.), Lithosphere Dynamics and Sedimentary Basins: The Arabian Plate and Analogues, Frontiers in Earth Sciences, p. 239-258, DOI: https://doi.org/10.1007/978-3-642-30609-9_12, Springer-Verlag Berlin Heidelberg

Butler, R.F., Gehrels, G.E., Kodama, K.P., 2001. A moderate translation alternative to the Baja British Columbia hypothesis. GSA Today 11, 4–10.

Calvert, A.J., Ramachandran, K., Kao, H., Fisher, M.A., 2006. Local thickening of the Cascadia forearc crust and the origin of seismic reflectors in the uppermost mantle. Tectonophysics 420 (1), 175–188.

Calvert, A.J., Preston, L.A., Farahbod, A.M., 2011. Sedimentary underplating at the Cascadia mantle-wedge corner revealed by seismic imaging. Nat. Geosci. 4 (8), 545.

Chapman, A.D., 2017. The Pelona–Orocopia–Rand and related schists of southern California: a review of the best-known archive of shallow subduction on the planet. Int. Geol. Rev. 59 (5–6), 664–701.

Chapman, A.D., Kidder, S., Saleeby, J.B., Ducea, M.N., 2010. Role of extrusion of the Rand and Sierra de Salinas schists in late cretaceous extension and rotation of the southern Sierra Nevada and vicinity. Tectonics 29 (5), TC5006.

Chapman, A.D., Luffi, P., Saleeby, J., Petersen, S., 2011. Metamorphic evolution, partial melting, and rapid exhumation above an ancient flat slab: insights from the san Emigdio schist, southern California. J. Metamorph. Geol. 29 (6), 601.

Chapman, A.D., Saleeby, J.B., Wood, D.J., Piasecki, A., Farley, K.A., Kidder, S., Ducea, M.N., 2012. Late cretaceous gravitational collapse of the southern Sierra Nevada batholith, California. Geosphere 8, 314–341.

Chapman, A.D., Saleeby, J.B., Eiler, J.M., 2013. Slab flattening trigger for isotopic disturbance and magmatic flare-up in the southernmost Sierra Nevada batholith, California. Geology 41, 1007–1010.

Chapman, A.D., Ducea, M.N., Kidder, S., Petrescu, L., 2014. Geochemical constraints on the petrogenesis of the Salinian arc, Central California: implications for the origin of intermediate magmas. Lithos 200-201, 126–141.

Chapman, A.D., Jacobson, C.E., Ernst, W.G., Grove, M., Dumitru, T., Hourigan, J., Ducea, M., 2016. Assembling the world's type shallow subduction complex: detrital zircon geochronologic constraints on the origin of the Nacimiento block, Central California coast ranges. Geosphere 12 (2), 1–25.

Chapman, A.D., Wood, D.J., Saleeby, J.B., Saleeby, Z., 2017a. Late cretaceous to early Neogene tectonic development of the southern Sierra Nevada region, California. Geological Society of America Field Guides 45, 187–228.

Chapman, J.B., Ducea, M.N., Kapp, P., Gehrels, G.E., Decelles, P.G., 2017b. Spatial and temporal radiogenic isotopic trends of magmatism in cordilleran orogens. Gondwana Res. 48, 189–204.

Cheadle, M.J., Czuchra, B.L., Byrne, T., Ando, C.J., Oliver, J.E., Brown, L.D., Kaufman, S., Malin, P.E., Phinney, R.A., 1986. The deep crustal structure of the Mojave Desert, California, from COCORP seismic reflection data. Tectonics 5, 293–320.

Chin, E.J., Lee, C.T., Tollstrup, D.L., Xie, L.W., Wimpenny, J.B., Yin, Q.Z., 2013. On the origin of hot metasedimentary quartzites in the lower crust. Earth Planet. Sci. Lett. 361, 120–133.

Clift, P., Vannucchi, P., 2004. Controls on tectonic accretion versus erosion in subduction zones: implications for the origin and recycling of the continental crust. Rev. Geophys. 42, RG2001.

Clift, P.D., Vannucchi, P., Morgan, J.P., 2009. Crustal redistribution, crust-mantle recycling and Phanerozoic evolution of the continental crust. Earth-Sci. Rev. 97, 80–104.

Cloos, M., 1982. Flow mélanges: numerical modeling and geologic constraints on their origin in the Franciscan subduction complex, California. Geol. Soc. Am. Bull. 93, 330–345.

Cloos, M., Shreve, L., 1988. Subduction-channel model of prism accretion, melange formation, sediment subduction, and subduction erosion at convergent plate margins. Pure Appl. Geophys. 128, 455–500.

Crouch, J.K., Suppe, J., 1993. Late Cenozoic tectonic evolution of the Los Angeles Basin and inner California borderland; a model for core complex–like crustal extension. Geol. Soc. Am. Bull. 105, 1415–1434.

Davidson, C., Garver, G.I., 2017. Age and origin of the resurrection ophiolite and associated Turbidites of the Chugach–Prince William terrane, Kenai peninsula, Alaska. The Journal of Geology 125, 681–700.

Dawson, M.R., Jacobson, C.E., 1989. Geochemistry and origin of mafic rocks from the Pelona, Orocopia, and Rand schists, southern-California. Earth Planet. Sci. Lett. 92, 371–385.

Decelles, P.G., 2004. Late Jurassic to Eocene evolution of the cordilleran thrust belt and foreland basin system, western U.S.A. American Journal of Sciences 304, 105–168.

Decelles, P.G., Robinson, D.M., Zandt, G., 2002. Implications of shortening in the Himalayan fold-thrust belt for uplift of the Tibetan Plateau, Tectonics, 21, Paper. 1062https://doi.org/10.1029/2001TC001322.

Decelles, P.G., Ducea, M.N., Kapp, P., Zandt, G., 2009. Cyclicity in cordilleran orogenic systems. Nat. Geosci. 2, 251–257.

Defant, M.J., Drummond, M.S., 1990. Derivation of some modern arc magmas by melting of young subducted lithosphere. Nature 347, 662–665.

Dektar, E., Chapman, A.D., 2018. Detrital zircon geochronology of blueschist facies sequences in the accretionary complex of west-Central Baja California, Mexico. Abstracts with programs - Geological Society of America 50 (5).

Dewey, J.F., 1988. Extensional collapse of orogens. Tectonics 7, 1123–1139.

Dibblee Jr., T.W., 1972. Rinconada fault in the southern Coast Ranges, California, and its significance. Geol. Soc. America, Abs. with Programs (Cordilleran Sec.) 4 (3), 145–146.

Dickinson, W.R., 1983. Cretaceous sinistral strike slip along the Nacimiento fault in coastal California. Am. Assoc. Pet. Geol. Bull. 67, 624–645.

Dickinson, W.R., Ducea, M., Rosenberg, L.I., Greene, H.G., Graham, S.A., Clark, J.C., Weber, G.E., Kidder, S., Ernst, W.G., Brabb, E.E., 2005. Net dextral slip, Neogene San Gregorio–Hosgri fault zone, coastal California: geologic evidence and tectonic implications. Geological Society of America Special Paper 391, 1–43.

Ducea, M.N., 2001. The California Arc; thick granitic batholiths, eclogitic residues, lithospheric- scale thrusting, and magmatic flare-ups. GSA Today 11, 4–10.

Ducea, M.N., 2002. Constraints on the bulk composition and root foundering rates of continental arcs; a California arc perspective. Journal of Geophysical Research, Solid Earth 107, B112304.

Ducea, M.N., Kidder, S., Zandt, G., 2003a. Arc composition at mid-crustal depths; insights from the coast Ridge Belt, Santa Lucia Mountains, California. Geophys. Res. Lett. 30, 1703–1707.

Ducea, M.N., Ganguly, J., Rosenberg, E., Patchett, P.J., Cheng, W., Isachsen, C., 2003b. Sm-Nd dating of spatially controlled domains of garnet single crystals. A new method of high temperature thermochronology: Earth and Planetary Science Letters 213, 31–42.

Ducea, M.N., House, M., Kidder, S., 2003c. Late Cenozoic denudation, bedrock and surface uplift rates in the Santa Lucia Mountains, California. Geology 31 (2), 139–142.

Ducea, M.N., Shoemaker, S., Gehrels, G.E., Ruiz, J., 2004a. The geologic development of the Xolapa arc, southern Mexico; evidence from U-Pb geochronology. Geol. Soc. Am. Bull. 116, 1016–1025.

Ducea, M.N., Valencia, V.A., Shoemaker, S., Reiners, P.W., Decelles, P., Moran-Zenteno, D.J., Campa, M.F., Ruiz, J., 2004b. Rates of sediment recycling beneath the Acapulco trench: constraints from (U-Th)/he Thermochronology. Journal of Geophysical

Research, Solid Earth 109 (B9).
Ducea, M.N., Kidder, S., Chesley, J.T., 2007. A geologic window into a subduction megathrust. Eos, Transactions, American Geophysical Union 88, 277–278.
Ducea, M.N., Kidder, S., Chesley, J.T., Saleeby, J., 2009. Tectonic underplating of trench sediments beneath magmatic arcs: the Central California example. Int. Geol. Rev. 51, 1–26.
Ducea, M.N., Saleeby, J.B., Bergantz, G., 2015. The architecture, chemistry, and evolution of continental magmatic arcs. In: Jeanloz, R., Freeman, K.H. (Eds.), Annual Review of Earth and Planetary Sciences. 43. pp. 299–331.
Dumitru, T.A., Gans, P.B., Foster, D.A., Miller, E.L., 1991. Refrigeration of the western Cordilleran lithosphere during Laramide shallow-angle subduction. Geology 19, 1145–1148.
Dusel-Bacon, C., Csejtey Jr., B., Foster, H.L., Doyle, E.O., Nokleberg, W.J., Plafker, G., 1993. Distribution, facies, ages, and proposed tectonic associations of regionally metamorphosed rocks in east- and south-Central Alaska. U.S. Geological Survey Professional Paper 1497-C, 73.
Dzierma, Y., Thorwart, M.M., Rabbel, W., Flueh, E.R., Alvarado, G.E., Mora, M.M., 2010. Imaging crustal structure in south Central Costa Rica with receiver functions. Geochem. Geophys. Geosyst. 11 (8).
Ehlig, P.L., 1981. Origin and tectonic history of the basement terrane of the San Gabriel Mountains, central Transverse Ranges. In: Ernst, W.G. (Ed.), The Geotectonic Development of California, Rubey Volume I. New Jersey, PrenticeHall, pp. 253–283.
Ernst, W.G., 1980. Mineral paragenesis in Franciscan metagraywackes of the Nacimiento Block, a subduction complex of the Southern California Coast Ranges. J. Geophys. Res. 85, 7045–7055.
Ferrari, L., Orozco-Esquivel, T., Manea, V., Manea, M., 2012. The dynamic history of the Trans-Mexican Volcanic Belt and the Mexico subduction zone. Tectonophysics 522, 122–149.
Garver, J.I., Davidson, C.M., 2015. Southwestern Laurentian zircons in upper cretaceous flysch of the Chugach–Prince William terrane in Alaska. Am. J. Sci. 315, 537–556.
Gehrels, G., 2014. Detrital zircon U-Pb geochronology applied to tectonics. Annu. Rev. Earth Planet. Sci. 42, 127–149.
Gehrels, G.E., Rushmore, M., Woodsworth, G., Crawford, M., Andronicos, C., Hollister, L., Patchett, P.J., Ducea, M.N., Butler, R., Klepeis, K., Davidson, C., Friedman, R., Haggart, J., Mahoney, B., Crawford, W., Pearson, D., Girardi, J., 2009. U-Pb geochronology of the Coast Mountains Batholith in north-coastal British Columbia: constraints on age and tectonic evolution. Geol. Soc. Am. Bull. 121, 1341–1361.
Girardi, J.D., Patchett, P.J., Ducea, M.N., Gehrels, G.E., Cecil, M.R., Rusmore, M.E., Woodsworth, G.J., Pearson, D.M., Manthei, C., Wetmore, P., 2012. Elemental and isotopic evidence for granitoid genesis from deep-seated sources in the Coast Mountains Batholith, British Columbia. J. Petrol. 53 (7), 1505–1536.
Gómez-Tuena, A., Mori, L., Straub, S.M., 2018. Geochemical and petrological insights into the tectonic origin of the Transmexican Volcanic Belt. Earth Sci. Rev. 183, 153–181. https://doi.org/10.1016/j.earscirev.2016.12.006.
Gordon, S.M., Miller, R.B., Sauer, K.B., 2017. Incorporation of sedimentary rocks into the deep levels of continental magmatic arcs: Links between the North Cascades arc and surrounding sedimentary terranes. From the Puget Lowland to East of the Cascade Range: Geologic Excursions in the Pacific Northwest. The Geological Society of America Field Guide 49, 101.
Gotberg, N., McQuarrie, N., Caillaux, V.C., 2010. Comparison of crustal thickening budget and shortening estimates in southern Peru (12–14 degrees S): implications for mass balance and rotations in the “Bolivian orocline”. Geol. Soc. Am. Bull. 122, 727–742.
Graham, C.M., Powell, R., 1984. A garnet-hornblende geothermometer: calibration, testing, and application to the Pelona schist, southern California. J. Metamorph. Geol. 2, 13–31.
Grove, M., Jacobson, C.E., Barth, A.P., Vucic, A., 2003a. Temporal and spatial trends of late cretaceous-early tertiary underplating Pelona and related schist beneath Southern California and southwestern Arizona. Special Papers Geological Social American 374, 381–406.
Grove, M., Lovera, O.M., Harrison, T.M., 2003b. Late Cretaceous cooling of the east-central Peninsular Ranges Batholith (33 degrees N); relationship to La Posta pluton emplacement, Laramide shallow subduction, and forearc. In: Johnson, S.E. (Ed.), Tectonic Evolution of Northwestern Mexico and the Southwestern USA. Geological Society of America Special Paper. 374. pp. 355–379.
Grove, M., Bebout, G.E., Jacobson, C.E., Barth, A.P., Kimbrough, D.L., King, R.L., Zou, H., Lovera, O.M., Mahoney, B.J., Gehrels, G.G., 2008. The Catalina schist: evidence for middle cretaceous subduction erosion of southwestern North America. In: Draut, A.E., Clift, P.D., Scholl, D.W. (Eds.), Formation and Applications of the Sedimentary Record in Arc Collision Zones. Vol. 436. Geological Society of America Special Paper, pp. 335–362.
Hacker, B.R., Abers, G.A., Peacock, S.M., 2003. Subduction Factory 1. Theoretical mineralogy, density, seismic wave speeds, and H_2O content. Journal of Geophysical Research, Solid Earth 108, B12029.
Haeussler, P.J., Bradley, D.C., Wells, R.E., Miller, M.L., 2003. Life and death of the resurrection plate: evidence for its existence and subduction in the northeastern Pacific in Paleocene-Eocene time. Geol. Soc. Am. Bull. 115, 867–880.
Hall Jr., C.A., 1991. Geology of the point Sur-Lopez point region, coast ranges, California; a part of the Southern California allochthon. Special Papers Geological Society of America 266, 40.
Hall, C.A., Saleeby, J.B., 2013. Salinia revisited: a crystalline nappe sequence lying above the Nacimiento fault and dispersed along the San Andreas fault system, Central California. Int. Geol. Rev. 55 (13), 1575–1615.
Haxel, G., Dillon, J., 1978. The Pelona Orocopia Schist and Vincent–Chocolate Mountain thrust system, Southern California. In: Howell, D.G., McDougall, K.A. (Eds.), Mesozoic Paleogeography of the Western United States: Pacific Section. Vol. 2. Society of Economic Paleontologists and Mineralogists Pacific Coast Paleogeography Symposium, pp. 453–469.
Haxel, G.B., Jacobson, C.E., Richard, S.M., Tosdal, R.M., Grubensky, M.J., 2002. The Orocopia Schist in southwest Arizona: Early Tertiary oceanic rocks trapped or transported far inland. In: Barth, A. (Ed.), Contributions to Crustal Evolution of the Southwestern United States. Vol. 365. Geological Society of America Special Paper, pp. 99–128.
Haxel, G.B., Jacobson, C.E., Wittke, J.H., 2015. Mantle peridotite in newly discovered far inland subduction complex, Southwest Arizona: initial report. Int. Geol. Rev. 57, 871–892.
Hsü, K.J., 1968. The principles of mélanges and their bearing on the Franciscan-Knoxville paradox. Geol. Soc. Am. Bull. 79, 1063–1074.
Ingersoll, R.V., Rumelhart, P.E., 1999. Three-stage evolution of the Los Angeles Basin, Southern California. Geology 27, 593–596.
Jacobson, C.E., 1983. Structural geology of the Pelona schist and Vincent thrust, San Gabriel Mountains, California. Geol. Soc. Am. Bull. 94 (6), 753–767.
Jacobson, C.E., 1995. Qualitative thermobarometry of inverted metamorphism in the Pelona and Rand schists, southern California, using calciferous amphibole in mafic schist. J. Metamorph. Geol. 13 (1), 79–92.
Jacobson, C.E., 1997. Metamorphic convergence of the upper and lower plates of the Vincent thrust, San Gabriel Mountains, southern California, USA. J. Metamorph. Geol. 15, 155–165.
Jacobson, C.E., Grove, M., Vucic, A., Pedrick, J.N., Ebert, K.A., 2007. Exhumation of the Orocopia schist and associated rocks of southeastern California: relative roles of erosion, synsubduction tectonic denudation, and middle Cenozoic extension. Geological Society of America Special Paper 419, 1–37.
Jacobson, C.E., Grove, M., Pedrick, J.N., Barth, A.P., Marsaglia, K.M., Gehrels, G.E., Nourse, J.A., 2011. Late cretaceous–early Cenozoic evolution of the southern California margin inferred from provenance of trench and forearc sediments. Geol. Soc. Am. Bull. 123 (3–4), 485–506.
Jacobson, C.E., Hourigan, J., Haxel, G.B., Grove, M.J., Hoyt, J.J., 2015. Orocopia schist at Cemetery Ridge, Arizona: A type exposure of subducted rocks accreted during Laramide flat subduction, then incorporated into a Miocene Cordilleran core complex. Abstracts with programs. Geological Society of America 47 (7), 432.
Johnson, T.E., White, R.W., Powell, R., 2008. Partial melting of metagreywacke: a calculated mineral equilibria study. J. Metamorph. Geol. 26, 837–853.
Johnston, S.M., Kylander-Clark, A.R.C., Chapman, A.D., 2018. Detrital Zircon Geochronology and Evolution of the Nacimiento Block Late Mesozoic Forearc Basin, Central California Coast. (Submitted to GSA Special Papers in press).
Jull, M., Kelemen, P.B., 2001. On the conditions for lower crustal convective instability. Journal of Geophysical Research, Solid Earth 106, 6423–6446.
Kay, S.M., Godoy, E., Kurtz, A., 2005. Episodic arc migration, crustal thickening, subduction erosion, and magmatism in the south-Central Andes. Geol. Soc. Am. Bull. 117, 67–88.
Kelemen, P.B., Hanghoj, K., Greene, A.R., 2004. One view of the geochemistry of subduction-related magmatic arcs, with an emphasis on primitive andesite and lower crust. In: Holland, H.D., Turekian, K.K. (Eds.), Treatise on Geochemistry. 3. Elsevier, Amsterdam, pp. 593–659.
Kellogg, K.S., Miggins, D.P., 2002. Geologic map of the Sawmill Mountain Quadrangle, Kern and Ventura Counties, California (Version 1.0). (U.S. Geological Survey Open-File Report 02-406).
Kidder, S., Ducea, M.N., 2006. High temperatures and inverted metamorphism in the schist of sierra de Salinas, California. Earth Planet. Sci. Lett. 241, 422–437.
Kidder, S., Ducea, M., Gehrels, G.E., Patchett, P.J., Vervoort, J., 2003. Tectonic and magmatic development of the Salinian Coast Ridge Belt, California. Tectonics 22 (5).
Kidder, S.B., Herman, F., Saleeby, J., Avouac, J.-P., Ducea, M.N., Chapman, A.D., 2013. Shear heating not a cause of inverted metamorphism. Geology 41, 899–902.
Kim, Y., Clayton, R.W., Asimow, P.D., Jackson, J.M., 2013. Generation of talc in the mantle wedge and its role in subduction dynamics in Central Mexico. Earth Planet. Sci. Lett. 384, 81–87. https://doi.org/10.1016/j.epsl.2013.10.006.
Kochelek, E.J., Amato, J.M., Pavlis, T.L., Clift, P.D., 2011. Flysch deposition and preservation of coherent bedding in an accretionary complex: detrital zircon ages from the upper cretaceous Valdez group, Chugach terrane, Alaska. Lithosphere 3 (4), 265–274.
Li, Y.-G., Henyey, T.L., Silver, L.T., 1992. Aspects of the crustal structure of the western Mojave Desert, California, from seismic-reflection and gravity-data. J. Geophys. Res. 97, 8805–8816.
Li, Z.H., Xu, Z.Q., Gerya, T.V., 2011. Flat versus steep subduction: contrasting modes for the formation and exhumation of high-to ultrahigh-pressure rocks in continental collision zones. Earth Planet. Sci. Lett. 301 (1–2), 65–77.
Liu, L., 2015. The ups and downs of North America: evaluating the role of mantle dynamic topography since the Mesozoic. Rev. Geophys. 53 (3), 1022–1049.
Liu, L., Gurnis, M., Seton, M., Saleeby, J., Müller, R.D., Jackson, J., 2010. The role of oceanic plateau subduction in the Laramide orogeny. Nat. Geosci. 3, 353–357.
Magistrale, H., Zhou, H., 1996. Lithologic control of the depth of earthquakes in southern California. Science 273, 639–642.
Malin, P.E., Goodman, E.D., Henyey, T.L., Li, Y.G., Okaya, D.A., Saleeby, J.B., 1995. Significance of seismic reflections beneath a tilted exposure of deep continental-crust, Tehachapi Mountains. California. J. Geophys. Res. 100, 2069–2087.
Manea, V.C., Manea, M., Ferrari, L., 2013. A geodynamical perspective on the subduction of Cocos and Rivera plates beneath Mexico and Central America. Tectonophysics 609, 56–81.
Matzel, J.E.P., Bowring, S.A., Miller, R.B., 2004. Protolith age of the Swakane Gneiss, North Cascades, Washington: evidence of rapid underthrusting of sediments beneath an arc. Tectonics 23 (6).
Melbourne, T., Webb, F.H., 2003. Slow but not quite silent. Science 300, 1886–1887.
Melgar, D., Pérez-Campos, X., 2011. Imaging the Moho and subducted oceanic crust at the

isthmus of Tehuantepec, Mexico, from receiver functions. Pure Appl. Geophys. 168 (8–9), 1449–1460.
Miller, J.S., Glazner, A.F., Crowe, D.E., 1996. Muscovite-garnet granites in the Mojave Desert: relation to crustal structure of the Cretaceous arc. Geology 24 (4), 335–338.
Miyashiro, A., 1973. Metamorphism and Metamorphic Belts. 492 George Allen and Unwin Ltd., London.
Moore, J.C., Diebold, J., Sample, J., et al., 1991. Edge deep seismic-reflection transect of the eastern Aleutian arc-trench layered lower crust reveals underplating and continental growth. Geology 19, 420–424.
Morán-Zenteno, D.J., Martiny, B.M., Solari, L., Mori, L., Luna-González, L., González-Torres, E.A., 2018. Cenozoic magmatism of the Sierra Madre del Sur and tectonic truncation of the Pacific margin of southern Mexico. Earth Sci. Rev. 183, 85–114.
Narcía-López, C., Castro, R.R., Rebollar, C.J., 2004. Determination of crustal thickness beneath Chiapas, Mexico using S and Sp waves. Geophys. J. Int. 157 (1), 215–228.
Oyarzabal, F.R., Jacobson, C.E., Haxel, G.B., 1997. Extensional reactivation of the Chocolate Mountains subduction thrust in the Gavilan Hills of southeastern California. Tectonics 16, 650–661.
Park, J.O., Tsuru, T., Takahashi, N., Hori, T., Kodaira, S., Nakanishi, A., Miura, S., Kaneda, Y., 2002. A deep strong reflector in the Nankai accretionary wedge from multichannel seismic data: implications for underplating and interseismic shear stress release. J. Geophys. Res. Solid Earth 107, 2061. (Article Number). https://doi.org/10.1029/2001JB000262.
Parolari, M., Gómez-Tuena, A., Cavazos-Tovar, J.G., Hernández-Quevedo, G., 2018. A balancing act of crust creation and destruction along the western. Mexican convergent margin: Geology 46, 455–458. https://doi.org/10.1130/G39972.1.
Peacock, S.M., 1987. Thermal effects of metamorphic fluids in subduction zones. Geology 15, 1057–1060.
Pearson, D.M., MacLeod, D.R., Ducea, M.N., Gehrels, G.E., Patchett, P.J., 2017. Sediment underthrusting within a continental magmatic arc: Coast Mountains batholith, British Columbia. Tectonics 36, 2022–2043.
Pérez-Campos, X., Kim, Y., Husker, A., Davis, P.M., Clayton, R.W., Iglesias, A., Pacheco, J.F., Singh, S.K., Manea, V.C., Gurnis, M., 2008. Horizontal subduction and truncation of the Cocos Plate beneath central Mexico. Geophys. Res. Lett. 35, L18303.
Philpotts, A., Ague, J., 2009. Principles of Igneous and Metamorphic Petrology. Cambridge University Press.
Platt, J.P., 1986. Dynamics of orogenic wedges and the uplift of high pressure metamorphic rocks. Geol. Soc. Am. Bull. 97, 1037–1053.
Porter, R., Zandt, G., McQuarrie, N., 2011. Pervasive lower- crustal seismic anisotropy in Southern California: evidence for underplated schists and active tectonics. Lithosphere 3, 201–220.
Postlethwaite, C.E., Jacobson, C.E., 1987. Early history and reactivation of the Rand thrust, southern California. J. Struct. Geol. 9 (2), 195–205.
Quinn, D.P., Saleeby, J., Ducea, M., Luffi, P., Asimow, P., 2018. Late-Cretaceous construction of the mantle lithosphere beneath the central California coast revealed by Crystal Knob xenoliths. Geochemistry, Geophysics, Geosystems. https://doi.org/10.1029/2017GC007260.
Raymond, L.A., 1984. Classification of mélanges. In: Raymond, L.A. (Ed.), Mélanges: Their Nature, Origins, and Significance. Vol. 198. Geological Society of America Special Paper, pp. 7–20.
Reguzzoni, M., Sampietro, D., 2012. Moho estimation using GOCE data: a numerical simulation. In: Geodesy for Planet Earth. Springer, Berlin, Heidelberg, pp. 205–214.
Rey, P., Vanderhaeghe, O., Teyssier, C., 2001. Gravitational collapse of the continental crust: definition, regimes and modes. Tectonophysics 342, 435–449.
Reymer, A., Schubert, G., 1984. Phanerozoic addition rates to the continental crust and crustal growth. Tectonics 3 (1), 63–77.
Ross, D.C., 1976. Metagraywacke in the Salinian block, central coast ranges, California-and a possible correlative across the San Andreas fault. U.S. Geological Survey Journal of Research 5, 683–696.
Rudnick, R.L., Gao, S., 2014. Composition of the Continental Crust. In: Holland, H., Turekian, K. (Eds.), Treatise on Geochemistry, 2nd ed. 4. Elsevier, pp. 1–51.
Rusmore, M.E., Woodsworth, G.J., Gehrels, G.E., 2005. Two-stage exhumation of mid-crustal arc rocks, Coast Mountains, British Columbia. Tectonics 24 (5).
Saleeby, J., 2003. Segmentation of the Laramide slab: evidence from the southern Sierra Nevada region. Geol. Soc. Am. Bull. 115, 655–668.
Saleeby, J., Farley, K.A., Kistler, R.W., Fleck, R., 2007. Thermal evolution and exhumation of deep-level batholithic exposures, southernmost Sierra Nevada, California. In: Cloos, M., Carlson, W.D., Gilbert, M.C., Liou, J.G., Sorensen, S.S. (Eds.), Convergent Margin Terranes and Associated Regions: A Tribute to W.G. Ernst. 419. Geological Society of America Special Paper, pp. 39–66.
Sauer, K.B., Gordon, S.M., Miller, R.B., Vervoort, J.D., Fisher, C.M., 2017. Transfer of metasupracrustal rocks to mid-crustal depths in the North Cascades continental magmatic arc, Skagit Gneiss complex, Washington. Tectonics 36, 3254–3276.
Sauer, K.B., Gordon, S.M., Miller, R.B., Vervoort, J.D., Fisher, C.M., 2018. Provenance and metamorphism of the Swakane Gneiss: Implications for incorporation of sediment into the deep levels of the North Cascades continental magmatic arc. Lithosphere, Washington.
Scholl, D.W., von Huene, R., 2007. Crustal recycling at modern subduction zones applied to the past—Issues of growth and preservation of continental basement crust, mantle geochemistry, and supercontinent reconstruction. In: Hatcher Jr.R.D., Carlson, M.P., McBride, J.H., Martínez Catalán, J.R. (Eds.), 4-D Framework of Continental Crust: Geological Society of America Memoir 200, pp. 9–32. https://doi.org/10.1130/2007.1200(02.
Silver, L.T., Nourse, J., Jacobson, C., Wood, D.J., 1995. Penrose Conference Field Trip: Rand Mountains – S. (Sierra Nevada – Tehachapi Mountains).
Spencer, J.E., Richard, S.M., Reynolds, S.J., Miller, R.J., Shafiqullah, M., Gilbert, W.G., Grubensky, M.J., 1995. Spatial and temporal relationships between mid-tertiary magmatism and extension in southwestern Arizona. Journal of Geophysical Research: Solid Earth 100, 10321–10351.
Straub, S.M., Gomez-Tuena, A., Stuart, F.M., Zellmer, G.F., Espinasa-Perena, R., Cai, Y., Iizuka, Y., 2011. Formation of hybrid arc andesites beneath thick continental crust. Earth Planet. Sci. Lett. 303, 337–347. https://doi.org/10.1016/j.epsl.2011.01.013.
Straub, S.M., Gómez-Tuena, A., Bindeman, I.N., Bolge, L.L., Brandl, P.A., Espinasa-Perena, R., Solari, L., Stuart, F.M., Vannucchi, P., Zellmer, G.F., 2015. Crustal recycling by subduction erosion in the central Mexican Volcanic Belt. Geochim. Cosmochim. Acta 166, 29–52. https://doi.org/10.1016/j.gca.2015.06.001.
Strickland, E.D., Singleton, J.S., Haxel, G.B., 2018. Orocopia Schist in the northern Plomosa Mountains, west-central Arizona: A Laramide subduction complex exhumed in a Miocene metamorphic core complex. (Submitted to Lithosphere in press).
Tape, C., Liu, Q., Maggi, A., Tromp, J., 2009. Adjoint tomography of the Southern California crust. Science 325, 988–992.
Trehu, A.M., Wheeler, W.H.I.V., 1987. Seismic reflection profile across the Coast Ranges of central California— Morro Bay to the San Andreas fault: U.S. Geological Survey Miscellaneous Field Studies (Map 1920, 1 sheet).
Turcotte, D., Schubert, G., 2014. Geodynamics. Cambridge University Press (636 pages).
Ukar, E., 2012. Tectonic significance of low-temperature blueschist blocks in the Franciscan mélange at San Simeon, California. Tectonophysics 568-569, 154–169.
Van Buer, N.J., Brigham, K.M., Soto, P.M., 2016. Late cretaceous high-flux magmatism in the western Mojave Desert. Geol. Soc. Am. Abstr. Programs 48 (4).
Von Huene, R., Scholl, D.W., 1991. Observations at convergent margins concerning sediment subduction, subduction erosion, and the growth of continental crust. Rev. Geophys. 29, 279–316.
Wakabayashi, J., 2015. Anatomy of a subduction complex: Architecture of the Franciscan Complex, California, at multiple length and time scales. Int. Geol. Rev. 57, 669–746.
Wetmore, P.H., Ducea, M.N., 2011. Geochemical evidence of a near-surface history for source rocks of the central Coast Mountains Batholith, British Columbia. Int. Geol. Rev. 53, 230–260.
Wright, T.L., 1991. Structural geology and tectonic evolution of the Los Angeles Basin, California. In: Biddle, K.T. (Ed.), Active Margin Basins. American Association of Petroleum Geologists Memoir. Vol. 52. pp. 35–134.
Xia, H., Platt, J.P., 2017. Structural and rheological evolution of the Laramide subduction channel in southern California. Solid Earth 8, 379–403.
Yonkee, W.A., Weil, A.B., 2015. Tectonic evolution of the Sevier and Laramide belts within the north American cordillera orogenic system. Earth Sci. Rev. 150, 531–593.